

# The analytically tractable zoo of similarity-induced exceptional structures

Anton Montag,<sup>1,2,\*</sup> Jordan Isaacs,<sup>1,3</sup> Marcus Stålhammar,<sup>4,5,†</sup> and Flore K. Kunst<sup>1,2,‡</sup>

<sup>1</sup>*Max Planck Institute for the Science of Light, Staudtstraße 2, 91058 Erlangen, Germany*

<sup>2</sup>*Department of Physics, Friedrich-Alexander Universität Erlangen-Nürnberg, Staudtstraße 7, 91058 Erlangen, Germany*

<sup>3</sup>*University of Ottawa, 75 Laurier Ave E, Ottawa, Ontario K1N 6N5, Canada*

<sup>4</sup>*Institute for Theoretical Physics, Utrecht University,  
Princetonplein 5, 3584CC Utrecht, The Netherlands*

<sup>5</sup>*Department of Physics and Astronomy, Uppsala University, Uppsala, Sweden*

(Dated: August 5, 2025)

Exceptional points (EPs) are non-Hermitian spectral degeneracies marking a simultaneous coalescence of eigenvalues and eigenvectors. Despite the fact that multiband  $n$ -fold EPs (EPns) generically emerge as special points on manifolds of EPms, where  $m < n$ , EPns as well as their topological properties have hitherto been studied as isolated objects. In this work we address this issue and carefully map out the emerging properties of multifold exceptional structures in three and four dimensions under the influence of one or multiple generalized similarities, revealing diverse combinations of EPms in direct connection to EPns. We find that simply counting the number of constraints defining the EPns is not sufficient in the presence of similarities; the constraints can also be satisfied by the EPm-manifolds obeying certain spectral symmetries in the complex eigenvalue plane, reducing their dimension beyond what is expected from counting the number of constraints. Furthermore, the induced spectral symmetries not always allow for any EPm-manifold to emerge in  $n$ -band systems, making the plethora of exceptional structures deviate further from naive expectations. We illustrate our findings in simple periodic toy models. By relying on similarity relations instead of the less general symmetries, we simultaneously cover several physically relevant scenarios, ranging from optics and topoelectrical circuits, to open quantum systems. This makes our predictions highly relevant and broadly applicable in modern research, as well as experimentally viable within various branches of physics.

## I. INTRODUCTION

The past decade has marked the advent of non-Hermitian topological physics [1], expanding extensively on the previous utilization of non-Hermitian operators, which was largely focused on optics, where these operators are used to model gain and loss [2–4]. Although they violate fundamental laws of quantum mechanics, non-Hermitian operators may also serve as effective descriptions of open quantum systems [5–7], ultra-cold atomic setups [8], friction in mechanics [9], resistivity in electrical circuits [10, 11], and damping matrices in Liouvillian descriptions [12], to mention a few examples. The most profound differences from conventional Hermitian systems include the biorthogonal bulk-boundary correspondence [13–15], the non-Hermitian skin effect [8, 14, 16], and the generic appearance of exceptional points (EPs) in the complex eigenvalue spectrum [17]. The latter marks a simultaneous coalescence of eigenvalues and eigenvectors, leaving the corresponding operator at a Jordan normal form instead of a diagonal form [17]. Remarkably, the generic appearance of  $n$ -fold EPs (EPns) requires the tuning of  $2n - 2$  real parameters [1, 18–22], making them vastly more abundant than their Hermitian counterparts, which require the simultaneous tuning of  $n^2 - 1$

$[2(n^2 - 1)]$  real parameters in (non-)Hermitian systems. Consequently, EP2s appear in a stable fashion already in two dimensions, while three-dimensional (3D) systems may host embeddings of one-dimensional (1D) submanifolds of EP2s potentially taking the form of links [23–25] and knots [26–29]. The number of tuning constraints is often referred to as the codimension of the corresponding degeneracy.

Focus has recently been directed towards further reducing the codimension of EPns. This is commonly done by exposing the dynamical matrix, the non-Hermitian operator governing the evolution of the system, to certain symmetries [22]; parity-time ( $\mathcal{PT}$ ) symmetry is for instance known to reduce the codimension to  $n - 1$  [21, 22, 30–33], while the codimension of EPns induced by sublattice symmetry is  $n - 1$  ( $n$ ) if  $n$  is odd (even), thus making it depend on the parity of  $n$  [21, 22, 32]. Mathematically speaking, all the different non-Hermitian symmetries that reduce the codimension of EPns are merely special cases of one of three generalized similarity relations [34]. Although the symmetries, their generators and an appropriate basis must be chosen to physically interpret the EPns, their topological properties are captured already at the level of similarity relations, which are naturally carried over to the more physically relevant symmetries.

Even though stable EPns (when  $n > 2$ ) always appear as special points on manifolds of EPms,  $m < n$ , previous studies have almost exclusively treated EPns as isolated objects, meaning that little attention has been directed towards the concomitant less degenerate excep-

\* anton.montag@mpl.mpg.de

† marcus.backlund@physics.uu.se

‡ flore.kunst@mpl.mpg.de

tional structures. Motivated by this, in this work we map out the different exceptional structures appearing in non-Hermitian systems subject to pseudo-(anti-)Hermiticity and self skew-similarity in three and four dimensions, respectively, which are the perfect examples to show the hierarchy of exceptional structures of various dimensions and various orders. We find that the similarity-induced EP4s appearing in 3D pseudo-Hermitian four-band systems are not only accompanied by EP3 arcs and EP2 surfaces, but also by purely real or complex conjugate pairs of EP2 arcs. The similarity-induced EP4s appearing in four dimensional (4D) self skew-similar four-band systems on the other hand, are merely accompanied by two different EP2 surfaces, as the spectral constraint induced by the similarity forbids the emergence of EP3s of any kind. This highlights the importance of not only reading off the number of constraints associated to a certain exceptional structure, but to further analyze how the similarity-induced spectral constraints can be satisfied.

When subjecting a non-Hermitian matrix to two different similarity relations simultaneously, the third one necessarily follows, and the codimension of EP $n$ s is further reduced to  $\lfloor \frac{n}{2} \rfloor$ , with  $\lfloor x \rfloor$  denoting the integer part of  $x$  [35]. This induces even more exotic exceptional spectral features, which were recently uncovered for systems in two dimensions [35]. In addition to the above, we here unravel the exceptional structures induced by multiple similarities in three and four dimensions. We find EP6s and EP7s in 3D six- and seven-band models, respectively, while 4D eight- and nine-band models host EP8s and EP9s, respectively. These point-like structures are special points on a zoo of higher-dimensional manifolds of EPs of lower degeneracy, but, crucially, not all types of exceptional degeneracies are allowed by the similarity-induced spectral relations. The Abelian eigenvalue topology of these point-like EP $n$ s are classified in terms of resultant winding numbers, complementing the recently developed classification scheme of multifold EPs [36, 37].

Our work deepens the fundamental understanding of non-Hermitian topological band theory and multifold EP $n$ s, and forms the final chapter in the study of analytically tractable similarity-induced exceptional structures [21, 22, 30, 32, 34, 35, 38]. Our results can be used in several areas of modern physics research within both the classical and the quantum regime. Significant examples include, but are not limited to, optics and topological photonics, where EPs can be directly mapped out using single-photon interferometry [29, 39], and ultra-cold atomic setups [40].

The remainder of this article is organized as follows. We set the stage in Sec. II by showing how generalized similarities lower the codimension of EPs and induce intricate lower-order (less degenerate) exceptional structures between EP $n$ s in  $n$ -band systems. Further, we introduce generic minimal models, and show that the non-vanishing terms in the characteristic polynomial and the spectral symmetry are equivalent to the generalized similarity constraints. Sec. III provides the exceptional

spectral structure connecting EP4s induced by pseudo-(anti-)Hermiticity in three dimensions, while Sec. IV does the same for self skew-similar systems in four dimensions. We address exceptional structures induced by multiple simultaneous similarities in three and four dimensions in Sec. V. We show the generic connection between EP( $2n$ )s and EP( $2n + 1$ )s, and provide a classification of the Abelian eigenvalue topology of EP $n$ s induced by multiple similarities in terms of resultant winding numbers. We conclude and put our results in a wider perspective in Sec. VI. The appendices are devoted to technical results, where we prove in Appendix A the equality between similarity relations and spectral symmetries, map out the interesting Fermi structures accompanying the exceptional structures present in the models treated in the main text in Appendix B, and we fully uncover in Appendix C the exceptional structures present in 4D systems subject to multiple similarities.

## II. SIMILARITY-INDUCED MULTIFOLD EXCEPTIONAL POINTS

Matrix similarity relations are generalizations of symmetry relations, and are obtained by relaxing the unitarity constraint on symmetry generators. Despite being more general, the similarities enforce spectral relations whose EP-inducing properties are the same as for the symmetries [22, 34, 41]. We devote this section to a brief survey on this topic, by introducing matrix similarities in Sec. II A, and their EP-inducing properties in Sec. II B. Sec. II C shows that the exceptional structures induced by similarities can be illustrated using toy models derived from Frobenius companion matrices.

### A. Similarities in non-Hermitian systems

In previous work it was established that unitary symmetries of non-Hermitian systems, which are local in parameter space, reduce the codimension of EP $n$ s and that there are six such distinct symmetries [22]. Recent work by some of the authors of this paper has shown that these six unitary symmetries are special cases of three similarities: pseudo Hermiticity, pseudo anti-Hermiticity, and self skew-similarity [34]. Each similarity is defined in terms of an invertible generator, as listed in Table I. Different choices of generators amount to different allowed contributions to the dynamical matrix. Their interpretation depends on the specific generator chosen, but we will not focus on this and rather work out general features induced by the similarities. The generator is either constant, i.e., independent of the point in parameter space, in which case we call the similarity a global similarity, while a so-called parametric similarity depends on the momentum  $\mathbf{k}$ . All the following statements are true, regardless of whether a model has a global similarity or parametric similarity at every point in parameter space.

Table I. Definitions of generalized self-similarities symmetries

Similarity	Similarity constraint	Spectral constraint
pseudo-Hermiticity	$H(\mathbf{k}) = \eta H^\dagger(\mathbf{k}) \eta^{-1}$	$\{\lambda(\mathbf{k})\} = \{\lambda^*(\mathbf{k})\}$
pseudo anti-Hermiticity	$H(\mathbf{k}) = -\Gamma H^\dagger(\mathbf{k}) \Gamma^{-1}$	$\{\lambda(\mathbf{k})\} = \{-\lambda^*(\mathbf{k})\}$
self skew-similarity	$H(\mathbf{k}) = -S H(\mathbf{k}) S^{-1}$	$\{\lambda(\mathbf{k})\} = \{-\lambda(\mathbf{k})\}$

Here the operators  $\eta, \Gamma$  and  $S$  are invertible, and  $\eta$  and  $\Gamma$  are Hermitian.

Each similarity is closely connected to a specific *spectral symmetry*, cf. Table I, which follows immediately from the similarity relation. By constructing a parametric similarity generator for a dynamical matrix with a specific spectral symmetry, we show in Appendix A that *spectral symmetry implies similarity*. This results in the following statement: Iff a non-Hermitian finite-dimensional dynamical matrix fulfills the pseudo-Hermitian, anti pseudo-Hermitian, or self skew-similar similarity constraint, it has the spectral symmetry  $\{\lambda(\mathbf{k})\} = \{\lambda^*(\mathbf{k})\}$ ,  $\{\lambda(\mathbf{k})\} = \{-\lambda^*(\mathbf{k})\}$ , or  $\{\lambda(\mathbf{k})\} = \{-\lambda(\mathbf{k})\}$ , respectively, and vice versa. These spectral symmetries play a key role in the appearance of multifold EPs in lower dimensions.

### B. Similarity-induced exceptional points

To see how the similarities induce stable multifold EPs, we introduce the conditions for them to appear in generic systems. An  $n$ -band system exhibits an EP $n$  if and only if all terms except the leading one in the characteristic polynomial vanish. The coefficients of the characteristic polynomial can be expressed as sums of the determinant  $\det[H]$  and  $n - 2$  different traces  $\text{tr}[H^k]$ , with  $k = 2, \dots, n - 1$  [42]. We set  $\text{tr}[H] = 0$  without loss of generality throughout, since a finite trace of a dynamical matrix  $H$  does not change its rank. Both the determinant and the  $n - 2$  traces are generally complex for non-Hermitian systems. This amounts to  $2(n - 1)$  real constraints, which need to be simultaneously enforced to find an EP $n$  [22]. The number of constraints is referred to as the codimension of the EP $n$ .

Due to the spectral symmetries imposed by similarities, some of the constraints defining the emergence of EP $n$ s trivially hold as a consequence of the similarity. Thus, the codimension of EP $n$ s can be reduced by imposing generalized self-similarities on the system [34]. The remaining constraints for  $n$ -band systems are derived in Refs. 22 and 34, and are listed in Table II.

The multifold exceptional structures emerging in two dimensions have been systematically studied in Ref. [35], and amount to EP3s, EP4s and EP5s induced by unitary symmetries. The results generalize directly to the similarity-induced EP $n$ s in two dimensions, because the symmetries constitute special cases of those similarities.

### C. Minimal Frobenius companion models

The exceptional structures induced by similarities are highlighted by toy models below. Minimal models with a certain similarity will be constructed using the *Frobenius companion matrix*

$$H = \begin{pmatrix} 0 & 1 & 0 & \dots & 0 \\ 0 & \ddots & \ddots & \ddots & \vdots \\ \vdots & \ddots & \ddots & \ddots & 1 \\ 0 & \dots & 0 & 0 & 1 \\ a_0 & a_1 & \dots & a_{n-2} & 0 \end{pmatrix}, \quad (1)$$

where  $a_i \in \mathbb{C}$  in general [22, 36, 43, 44]. The characteristic polynomial is given by

$$P_n(\lambda) = (-1)^n \left( \lambda^n - \sum_{j=0}^{n-2} a_j \lambda^j \right). \quad (2)$$

The spectral symmetries enforced by the similarities impose constraints on the  $a_i$ , which are listed in Table II. Thus by imposing the constraints from Table II on the models we obtain toy models for all possible similarities according to the proof in Appendix A.

## III. EXCEPTIONAL STRUCTURES INDUCED BY PSEUDO HERMITICITY

EP $n$ s induced by pseudo-Hermiticity have hitherto to a large extent been studied as isolated objects, thus neglecting (or avoiding) the fact that these appear as special points of manifolds of less degenerate EPs. In this section we map out these exceptional structures, initially in 3D (Sec. III A) and include an example in Sec. III B before general conclusions are made (Sec. III C). We comment on pseudo anti-Hermiticity in Sec. III D.

### A. General considerations

It is known that EP4s emerge pairwise and in a stable fashion in pseudo-Hermitian 4-band systems in a 3D parameter space, and a topological classification of them was recently derived [36]. Here we study the exceptional structures between them and show that they comprise of EP2 surfaces, special arcs on those surfaces, and EP3 arcs connecting pairs of EP4s.

Let us show this in detail. Consider a general pseudo-Hermitian 4-band dynamical matrix  $H(\mathbf{k}) = \eta H^\dagger(\mathbf{k}) \eta^{-1}$ , shift it by a  $\mathbf{k}$  dependent constant such that  $\text{tr}[H(\mathbf{k})] = 0$ , and introduce

$$\alpha = -\frac{1}{6} \text{tr}(H^2), \quad (3)$$

$$\beta = -\frac{1}{3\sqrt{2}} \text{tr}(H^3), \quad (4)$$

Table II. Number of constraints for realizing EPns in  $n$ -band systems restricted by generalized self-similarities and constraints on the terms in the characteristic polynomials for similarity constrained models.

Similarity [spectrum]	# constraints/codimension		coefficients of characteristic polynomial	
	$n \in \text{even}$	$n \in \text{odd}$	$j = 0 \vee j \in \text{even}$	$j \in \text{odd}$
pseudo-Hermiticity [ $\{\lambda\} = \{\lambda^*\}$ ]	$n - 1 \begin{cases} \text{Re}[\det(\mathcal{H})], \\ \text{Re}[\text{tr}(\mathcal{H}^k)]. \end{cases}$	$n - 1 \begin{cases} \text{Re}[\det(\mathcal{H})], \\ \text{Re}[\text{tr}(\mathcal{H}^k)]. \end{cases}$	$a_j \in \mathbb{R}$	$a_j \in \mathbb{R}$
pseudo anti-Hermiticity [ $\{\lambda\} = \{-\lambda^*\}$ ]	$n - 1 \begin{cases} \text{Re}[\det(\mathcal{H})], \\ \text{Re}[\text{tr}(\mathcal{H}^l)], \\ \text{Im}[\text{tr}(\mathcal{H}^m)]. \end{cases}$	$n - 1 \begin{cases} \text{Im}[\det(\mathcal{H})], \\ \text{Re}[\text{tr}(\mathcal{H}^l)], \\ \text{Im}[\text{tr}(\mathcal{H}^m)]. \end{cases}$	$a_j \begin{cases} \in \mathbb{R} \text{ if } n \in \text{even}, \\ \in i\mathbb{R} \text{ if } n \in \text{odd} \end{cases}$	$a_j \begin{cases} \in i\mathbb{R} \text{ if } n \in \text{even}, \\ \in \mathbb{R} \text{ if } n \in \text{odd} \end{cases}$
self skew-similarity [ $\{\lambda\} = \{-\lambda\}$ ]	$n \begin{cases} \det(\mathcal{H}), \\ \text{tr}(\mathcal{H}^l). \end{cases}$	$n - 1 \begin{cases} \text{tr}(\mathcal{H}^l). \end{cases}$	$a_j \begin{cases} \in \mathbb{C} \text{ if } n \in \text{even}, \\ = 0 \text{ if } n \in \text{odd} \end{cases}$	$a_j \begin{cases} = 0 \text{ if } n \in \text{even}, \\ \in \mathbb{C} \text{ if } n \in \text{odd} \end{cases}$
combined <sup>1</sup> [ $\{\lambda\} = \{\lambda^*\} \wedge \{\lambda\} = \{-\lambda\}$ ]	$\frac{n}{2} \begin{cases} \text{Re}[\det(\mathcal{H})], \\ \text{Re}[\text{tr}(\mathcal{H}^l)]. \end{cases}$	$\frac{n-1}{2} \begin{cases} \text{Re}[\text{tr}(\mathcal{H}^l)]. \end{cases}$	$a_j \begin{cases} \in \mathbb{R} \text{ if } n \in \text{even}, \\ = 0 \text{ if } n \in \text{odd} \end{cases}$	$a_j \begin{cases} = 0 \text{ if } n \in \text{even}, \\ \in \mathbb{R} \text{ if } n \in \text{odd} \end{cases}$

Here  $k \in \{2, \dots, n-1\}$ ,  $l \in \{2 \leq l < n, l \in \text{even}\}$  and  $m \in \{3 \leq m < n, m \in \text{odd}\}$ . Behind the number of constraints we write the specific quantities that need to be set to zero to find EPns. <sup>1</sup>Here combined encompasses the constraints enforced by any pair of similarities above.

$$\gamma = \frac{4}{3} \det(H). \quad (5)$$

Using the pseudo-Hermiticity constraint we find that all three parameters  $\alpha, \beta, \gamma \in \mathbb{R}$  [22, 34] and thus the characteristic polynomial is a real fourth-order polynomial given by

$$\mathcal{P}_4(\lambda) = \lambda^4 + 3\alpha\lambda^2 + \sqrt{2}\beta\lambda + \frac{3}{4}\gamma. \quad (6)$$

The third-order term vanishes, because we are only considering traceless dynamical matrices [22]. The discriminant of this polynomial is given by

$$\mathcal{D}_4 = -108 (2\alpha^3\beta^2 + \beta^4 - 9\alpha^4\gamma - 6\alpha\beta^2\gamma + 6\alpha^2\gamma^2 - \gamma^3). \quad (7)$$

The eigenvalues of a real fourth-order characteristic polynomial are either real or appear as complex conjugate pairs, thus fulfilling the spectral symmetry.

Since EPs appear at eigenvalue degeneracies, they correspond to points where the discriminant vanishes. Strictly speaking this is only a condition for finding spectral degeneracies, but since diabolic points, i.e., non-defective degeneracies or “Hermitian” degeneracies, require more constraints to be fulfilled [ $2(n^2 - 1)$  real constraints] they have higher codimension [31]. It is known that similarity-induced EP4s appear if and only if  $\alpha = \beta = \gamma = 0$  [22, 34]. When these constraints are met, they individually define closed surfaces in the periodic 3D parameter space, whose intersection are generically points appearing pairwise. This can be visualized by first considering the intersection between two of the three closed surfaces, which is a closed loop. If this loop intersects with the third surface there must be at least two points where all three constraints are fulfilled. Any additional intersection of the loop with the surface will lead to the emergence of another pair of EP4s. Apart from this geometric argument a doubling theorem based

on the resultant winding number of the EP4, generalizing to general EPns in  $n$ -band systems, has recently been derived [36].

Similar to similarity-induced EP3s in 2D parameter spaces we expect the EP4 pairs to be connected by exceptional structures of lower degeneracy. By rewriting the discriminant and setting it to zero, these structures arise as solutions to

$$\beta^2 [\beta^2 + 2(\alpha^3 - 3\alpha\gamma)] - \gamma(3\alpha^2 - \gamma)^2 = 0, \quad (8)$$

which results in the following:

- (i) Surfaces of real EP2s given by  $\mathcal{D}_4 = 0$  for  $\beta \neq 0$ , accompanied by two non-degenerate real or a pair of complex conjugate eigenvalues;
- (ii) Arcs along which pairs of purely real EP2s appear at the intersection of different EP2 surfaces. Both EP2s are similarity induced, but them appearing simultaneously results in the codimension of 2 associated with this structure;
- (iii) Arcs of real EP3s emerging on the EP2 surfaces;
- (iv) Arcs of complex conjugated pairs of purely imaginary EP2s appear connected to the remaining exceptional structure only at the EP4s. Their emergence is again not similarity-induced, and the similarity constraint instead results in the pairwise appearance.

Let us explain in detail how these EPs emerge in the following.

The real EP2s (i) emerge on two closed surfaces, where the isolated surfaces are defined by Eq. (8) for  $\beta \neq 0$ . The intersection of these surfaces, corresponding to  $\beta = 0$  and  $3\alpha^2 - \gamma = 0$  for  $\alpha < 0$ , defines a closed loop on which there is a pair of real EP2s (ii). Here two constraints need to be fulfilled, which can be interpreted as one constraint per



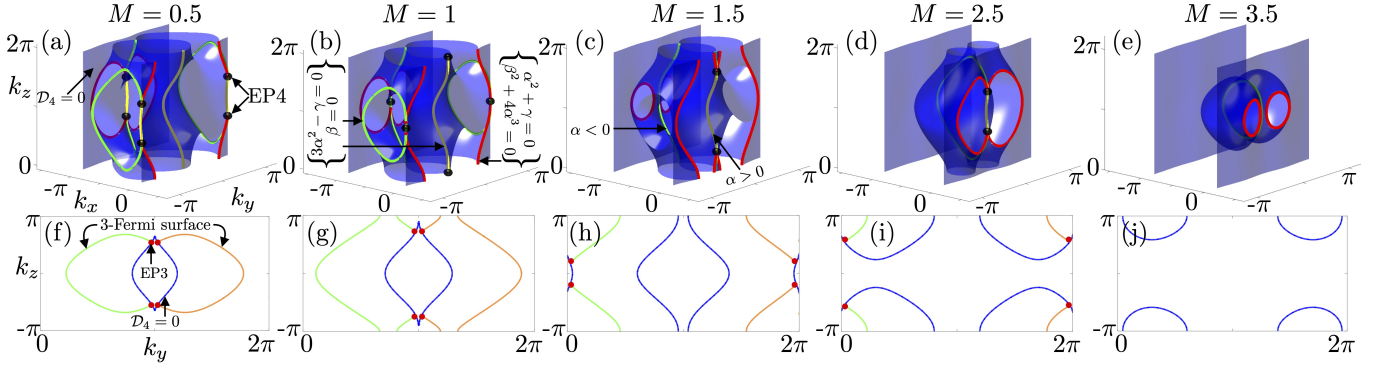


Figure 1. Exceptional structures of the pseudo-Hermitian 4-band model in 3D given by Eqs. (16)-(18) in panels (a)-(e), and their concomitant 3-level Fermi surfaces in for  $k_x = 0$  in panels (f)-(j). In panels (a)-(e), the blue surfaces are similarity-induced EP2s ( $\mathcal{D}_4 = 0$ ), the red arcs are similarity-induced EP3s ( $\alpha^2 + \gamma = \beta^2 + 4\alpha^3 = 0$ ), and the black dots are similarity-induced EP4s ( $\alpha = \beta = \gamma = 0$ ). The green and yellow arcs, however, denote special EP2s of codimension 2. The yellow (green) arcs arise as solutions to  $\beta = 3\alpha^2 - \gamma = 0$  with  $\alpha > 0$  ( $\alpha < 0$ ). Panels (a)-(e) display how the EP4s are pairwise created/annihilated as a function of the real parameter  $M$ , a process that affects the appearance of the similarity-induced EP3 arcs, but also the special EP2 arcs. In panels (f)-(j), the behavior of the 3-level Fermi surfaces (green and orange arcs), where three of the four eigenvalues share identical real parts, and the discriminant (blue arc) is displayed. The green and orange arcs correspond to 3-level Fermi surfaces given by Eq. (14) and Eq. (15), respectively. For illustrative purposes, this is displayed for a 2D cut of the Brillouin zone given by  $k_x = 0$ . The intersection of the 3-level Fermi surfaces with the discriminant forms EP3s (red dots), and when there are no intersections, the EP3s are gapped out, as shown in panel (j).

EP2. This loop connects to the EP4s at  $\alpha = \beta = \gamma = 0$ . The dimension of the real EP2 surface agrees with the expected dimensions from the codimension of EP2s in pseudo-Hermitian systems.

EP3s (iii) appear if  $\alpha^2 + \gamma = 0$  and  $\beta^2 + 4\alpha^3 = 0$ . These EP3 arcs emerge on the real EP2 surfaces. EP4 pairs are connected by two topologically distinct EP3 arcs. These are distinguished by the sign of the degenerate eigenvalue, or, equivalently, the sign of  $\beta$ . The codimension of the EP3 arcs is reflected in the number of constraints that must be fulfilled for the emergence of the EP3 arcs in pseudo-Hermitian systems.

Standing out slightly are the pairs of imaginary EP2 arcs (iv). These emerge for  $\beta = 0$  and  $3\alpha^2 - \gamma = 0$  with  $\alpha > 0$ , also connecting the EP4s at  $\alpha = \beta = \gamma = 0$ . The EP2s on these arcs have codimension 2, because two constraints need to be fulfilled for them to appear. Therefore they have a higher codimension than we expect of EP2s in pseudo-Hermitian systems. The reason for this is that these EP2 arcs are not similarity-induced, but rather ordinary EP2s with codimension 2. Instead of reducing the codimension, the spectral symmetry forces these imaginary EP2-arcs to come in complex conjugate pairs, leaving them to necessarily emerge with codimension 2.

No other EPs can emerge in the presence of pseudo-Hermiticity in a four band system. In addition to the exceptional structures, pseudo-Hermitian systems exhibit interesting Fermi structures, which in the case of four-band models form 3-level Fermi surfaces. At these, three of the four eigenvalues share the same real part while still being non-degenerate, a condition for which a closed-form expression can be derived analytically. By introducing

$u, v$  and  $w$  as,

$$\alpha = \frac{1}{3}(v + w - 4u^2), \quad (9)$$

$$\beta = \sqrt{2}u(w - v), \quad (10)$$

$$\gamma = \frac{4}{3}wv, \quad (11)$$

the characteristic polynomial can, by using Descartes method, be recast into the form

$$\mathcal{P}_4(\lambda) = (\lambda^2 + 2u\lambda + v)(\lambda^2 - 2u\lambda + 2). \quad (12)$$

The eigenvalue solutions  $\mathcal{P}_4(\lambda_{i,\pm}) = 0$  then read

$$\lambda_{1,\pm} = u \pm \sqrt{u^2 - v}, \quad \lambda_{2,\pm} = -u \pm \sqrt{u^2 - w}, \quad (13)$$

giving 3-level Fermi surfaces when the following conditions are met:

$$4u^2 = u^2 - v, \quad u^2 - w < 0, \quad (14)$$

$$4u^2 = u^2 - w, \quad u^2 - v < 0. \quad (15)$$

These are of importance since their intersections with the EP2 surface exactly form the EP3 arcs. The full Fermi structure of pseudo-Hermitian four band systems is highlighted in Appendix B.

## B. An example

To illustrate the exceptional spectral features, we consider the following example of a pseudo-Hermitian 4-band

model in a 3D parameter space given by

$$H_4 = \begin{pmatrix} 0 & 1 & 0 & 0 \\ 0 & 0 & 1 & 0 \\ 0 & 0 & 0 & 1 \\ a_0 & a_1 & a_2 & 0 \end{pmatrix}, \quad (16)$$

$$a_0 = \sin(k_x), \quad a_1 = \sin(k_y), \quad (17)$$

$$a_2 = M - \cos(k_x) - \cos(k_y) + \cos(k_z). \quad (18)$$

$k_x, k_y, k_z$  denote the lattice momentum components, and  $M$  is a real constant parameter. This model is inspired by the (Hermitian) Weyl semimetal model used in Ref. [45], and its eigenvalue structures are shown in Fig. 1. Figs. 1(a)-(e) show how the surfaces of similarity-induced EP2s (blue surfaces), the similarity-induced arcs of EP3s (red arcs), and the special EP2 arcs (yellow arcs are complex conjugated, and green arcs, corresponding to the intersection between the EP2 surfaces, are fully real) are all connected to the similarity-induced EP4s (black dots) in the way predicted above. Moreover, Fig. 1(f)-(i) shows the 3-level Fermi surfaces [green arc for Eq. (14), orange arc for Eq. (15)] and the vanishing of the discriminant (blue arc) in the cut  $k_x = 0$ . As claimed, their intersection form EP3s (red dots), and when their intersection is empty, no EP3s appear in the spectrum.

### C. Dimensional generalization

From the observations made in the special case presented in the previous subsection, we see that the pseudo-Hermitian similarity-induced EP structures are accompanied by some generic exceptional structures. Using these insights, we here identify the generic EP structures in the general case. To do this, we will treat the cases of even and odd bands separately.

When the matrix dimension  $n$  is even, a pseudo-Hermitian spectrum is achieved by an operator of the form

$$H = \begin{pmatrix} \mathcal{H} & 0 \\ 0 & \mathcal{H}^\dagger \end{pmatrix} \quad (19)$$

for some generic dynamical  $n/2 \times n/2$  matrix  $\mathcal{H}$ , and its conjugate transpose  $\mathcal{H}^\dagger$ . Since the corresponding spectrum satisfies the symmetries induced by pseudo-Hermitian similarity, we can by the proof in Appendix A conclude that such a matrix is pseudo-Hermitian with respect to some generator. Since  $\mathcal{H}$  is a generic matrix, i.e., it does not fulfill any similarity constraint, the exceptional structures appearing blockwise will not have a reduced codimension, but rather appear as generic exceptional structures. The spectral constraint induced by the similarity will instead ensure that these structures emerge either as complex conjugate paired structures, or as purely real structures; they either appear at purely real eigenvalues, or they appear pairwise in each half of the complex eigenvalues plane. This means that in addition

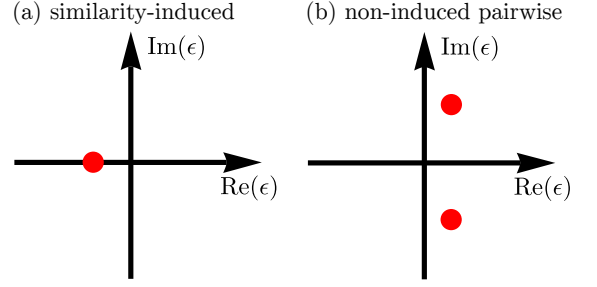


Figure 2. Illustration of how pseudo-Hermitian similarity constrains the position of exceptional structures of  $n$ -band systems (red dots) in the complex eigenvalue plane. (a) Similarity-induced EPms of codimension  $m-1$  are, when  $m \leq n$ , forced to appear at real eigenvalues. (b) Despite the similarity, EPms of order  $m \leq \lfloor \frac{n}{2} \rfloor$ , with  $\lfloor x \rfloor$  denoting the integer part of  $x$ , of generic codimension  $2m-2$  may still appear in the spectrum, but they are constrained to appear pairwise at complex conjugate eigenvalues.

to the similarity-induced structures of EPks of codimension  $k-1 < n$ , there will be generic structures of EPms with  $m \leq n/2$  of the generic codimension  $2m-2$ , which either are restricted to the real eigenvalue axis, or emerge at complex conjugate eigenvalues.

When  $n$  is odd, a pseudo-Hermitian spectrum is instead achieved by an operator on the form

$$H = \begin{pmatrix} \mathcal{H} & 0 & 0 \\ 0 & \mathcal{H}^\dagger & 0 \\ 0 & 0 & \lambda \end{pmatrix}, \quad (20)$$

where  $\mathcal{H}$  is again an  $(n-1)/2 \times (n-1)/2$  matrix representation of a generic operator  $\mathcal{H}$ , and  $\mathcal{H}^\dagger$  its conjugate transpose. Here,  $\lambda$  is necessarily real, as it comprises a pseudo-Hermitian eigenvalue whose conjugate does not appear in the rest of the spectrum. Here, the same reasoning as for the case of an even number of bands holds, meaning that the similarity-induced structures of EPks of codimension  $k-1 < n$  will be accompanied by generic structures of EPms with  $m \leq (n-1)/2$  of codimension  $2m-2$ , emerging at purely real or at complex conjugate eigenvalues.

To conclude, the spectrum of a pseudo-Hermitian operator not only hosts similarity-induced EPks of codimensions  $k-1$ , but also generic EPms of codimension  $2m-2$  when the number of bands is at least  $2m$ . Fig. 2 illustrates that these EPs are constrained to emerge at the real axis and at complex conjugate eigenvalues, respectively, to assure them fulfilling the similarity-induced spectral constraints.

### D. Pseudo anti-Hermiticity

The results in this section can be extended to pseudo anti-Hermitian systems in a straightforward manner: the exceptional structures for a pseudo anti-Hermitian sys-

tem  $\tilde{H}(\mathbf{k})$  are found by rotating those of a pseudo-Hermitian system  $H' = -i\tilde{H}$  by  $\pi/2$  in the complex plane. This means that any eigenvalue  $\lambda$  of  $H'$  is mapped to  $\tilde{\lambda} = -i\lambda$ , which is an eigenvalue of  $\tilde{H}$ . This shows that any exceptional point in the spectrum of  $\tilde{H}$  can be derived by considering the exceptional structure of  $H'$ . For four-band pseudo anti-Hermitian models in particular this implies the presence of pairs of EP4s, connected by surfaces of imaginary EP2s, intersecting in lines of paired imaginary EP2s and with EP3 lines emerging on them, and additional isolated arcs of non-induced paired real EP2s.

#### IV. SELF SKEW-SIMILARITY INDUCED EPNS

Self skew-similarity is different from the other two similarities, because it relates a dynamical matrix to itself and not its adjoint. This results in a unique structure of the similarity-constrained characteristic polynomial. Since it is the generalization of the (non-)Hermitian sublattice symmetry, which is present in many tight-binding models, self-skew similarity is of special importance. In these systems EPns emerge pairwise in  $n$  ( $n-1$ ) dimensions when  $n$  is even (odd), and they are topologically classified in Ref. [37]. Here we show that the corresponding eigenvalues can be derived by mapping  $2n$ - and  $(2n+1)$ -band self skew-similar models onto unconstrained  $n$ -band non-Hermitian models (Secs. IV A and IV B). We highlight with an example how the exceptional structure of self skew-similar systems can be obtained with this method (Sec. IV C).

##### A. Likeness of $2n$ and $2n+1$ models

The characteristic polynomials of a self skew-similar system with  $2n$  and  $2n+1$  bands are given by

$$n \in \text{even: } P_{2n}(\lambda) = \left( \lambda^{2n} - \sum_{j=0}^{n-1} a_{2j} \lambda^{2j} \right), \quad (21)$$

$$n \in \text{odd: } P_n(\lambda) = -\lambda \left( \lambda^{2n} - \sum_{j=0}^{n-1} a_{2j+1} \lambda^{2j} \right). \quad (22)$$

For an odd number of bands,  $\lambda = 0$  is thus always an eigenvalue of the system, appearing as a flat band. This implies the existence of compact localized non-decaying states. The form of the characteristic polynomial further makes it possible to achieve the spectral structure of a self skew-similar  $(2n+1)$ -band system by adding a flat band to the spectrum of a self skew-similar  $2n$ -band system by letting  $a_{2j+1} \rightarrow a_{2j}$ . We find similarity-induced EP2ns at  $\lambda = 0$  in  $2n$  dimensions, and since the flat band in the  $2n+1$ -band system is also at  $\lambda = 0$  the EPs are promoted to EP( $2n+1$ )s. The same argument holds for any exceptional structure of lower degeneracy

at  $\lambda = 0$ : any  $k$ -fold ( $k \leq 2n$ ) exceptional structure at  $\lambda = 0$  found in  $2n$ -band systems in the presence of self skew-similarity is promoted to a  $k+1$ -fold exceptional structure in  $2n+1$ -band systems. Further, all exceptional structures found in  $2n$ -band systems at  $\lambda \neq 0$  remain unaltered upon adding the  $(2n+1)$ th band. Therefore, studying the exceptional structures of self skew-similar  $2n$ -band systems also reveals the exceptional structure of self skew-similar systems with  $2n+1$  bands, which is why we from here on will consider self skew-similar systems with an even number of bands exclusively.

##### B. Mapping to unconstrained lower-band model

The form of the characteristic polynomial of  $2n$ -band self skew-similar systems can be mapped to that of a generic  $n$ -band system. Such a mapping will facilitate solving for the eigenvalues, and thus also finding the exceptional structures connected to the EP2ns. With the substitution

$$z = \lambda^2 - \frac{a_{2n-2}}{n} \quad (23)$$

the characteristic polynomial can be transformed to

$$\tilde{P}_n(z) = z^n - \sum_{j=0}^{n-2} b_j z^j, \quad (24)$$

where the coefficients  $b_j$  are complex-valued functions of  $a_0, \dots, a_{2n-2}$ . Given the solution for the  $n$  eigenvalues  $z_l$ , and by utilizing

$$\lambda_{\pm}(z_l) = \pm \sqrt{z_l + a_{2n-2}/n}, \quad (25)$$

the eigenvalues of the initial self skew-similar  $2n$ -band model can be derived. An identical principle can be used for systems subject to multiple similarities, which we will see in Sec. V.

##### C. An example

To exemplify the mapping and to highlight how the exceptional structure of higher-band self skew-similar systems can be solved using this method, we consider a self skew-similar 4-band model described by

$$H' = \begin{pmatrix} 0 & 1 & 0 & 0 \\ 0 & 0 & 1 & 0 \\ 0 & 0 & 0 & 1 \\ a_0 & 0 & a_2 & 0 \end{pmatrix}, \quad (26)$$

$$a_0 = \sin(k_x) + i \sin(k_y), \quad (27)$$

$$a_2 = \sin(k_z) + i \left[ M - \sum_{i=x,y,z} \cos(k_i) + \cos(k_w) \right], \quad (28)$$

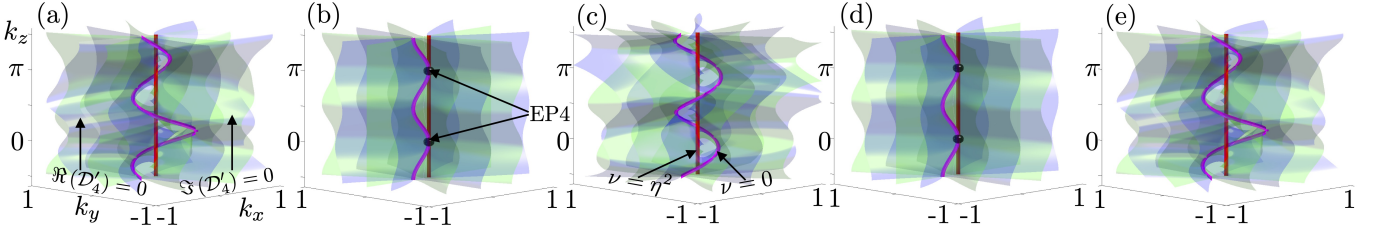


Figure 3. Exceptional structures in part of the Brillouin zone of the model given by Eqs. (26)-(28). The blue (green) surfaces correspond to the real (imaginary) part of the discriminant  $\mathcal{D}'_4$  of  $P'_4(\lambda)$  being zero, while the red (magenta) arcs illustrate the EP2 2D surfaces in 4D given by  $\nu = \eta^2$  ( $\nu = 0$ ) as 1D arcs in 3D. The panels (a)-(e) show different cuts in  $k_w$ , given by  $k_w = (-\frac{3k_0}{2}, -k_0, 0, k_0, \frac{3k_0}{2})$ , respectively, with  $k_0 = \cos^{-1} \left[ \sum_{i=x,y,z} \cos(k_i) - M \right]$ . When  $k_w = -k_0$  (b), and  $k_w = k_0$  (d), the system hosts EP4s appearing as intersections between the different EP2 structures, which do not appear when  $k_w = -\frac{3k_0}{2}$  (a),  $k_w = 0$  (c), or  $k_w = \frac{3k_0}{2}$  (e). Notable is further that the direction of winding of the magenta arc around the red arc changes when passing through the EP4s, something that can only occur through such a transition.

in a 4D space parametrized by  $(k_x, k_y, k_z, k_w)$ . As shown before all results obtained here can be transferred to a self skew-similar 5-band model by adding a flat band at the origin. Introducing

$$\eta = -\frac{\text{tr}[(H')^2]}{4}, \quad \nu = \det[H'] - \left\{ \frac{\text{tr}[(H')^2]}{4} \right\}^2, \quad (29)$$

we can write the characteristic polynomial as

$$P'_4(\lambda) = \lambda^4 + 2\eta\lambda^2 + \nu + \eta^2. \quad (30)$$

By substituting  $z = \lambda^2 + \eta$  the reduced polynomial is given by

$$\tilde{P}(z) = z^2 + \nu. \quad (31)$$

Similarity-induced EP4s are then found when  $\eta = \nu = 0$ . These EP4s are connected by different surfaces of EP2s, given by (i)  $\nu = 0, \eta \neq 0$ , and (ii)  $\nu = \eta^2$ . The constraint  $\nu = 0$  gives a pair of EP2 surfaces, connected at the EP4, while  $\nu = \eta^2$  gives an EP2 surface appearing at  $\lambda = 0$ , accompanied by two non-degenerate eigenvalues. Fig. 3 illustrates how these exceptional structure appear in different 3D slices. Consequently, the EP2s appear as arcs rather than surfaces, and the EP4s only appear in panels (b) and (d), corresponding to the slices in  $k_w$  including the EP4s. The fact that the EP2 arcs do not vanish regardless of the chosen  $k_w$ -slice, while the EP4s do, indicate that the EP2 structure is indeed a 2D surface embedded in 4D, while the EP4s are points in 4D.

These are the only exceptional structures emerging between the induced EP4s. Even though EP3s are expected to emerge in four dimensions the self skew-similarity prevents this for 4-band systems; with four bands it is impossible to have an EP3 and fulfill the spectral symmetry enforced by self skew-similarity. In addition to the exceptional structure we find Fermi structures for these systems, which are described in Appendix B.

Lastly, let us comment on how these exceptional structures are affected when adding a fifth band. Following the similarity constraints, this band is necessarily flat

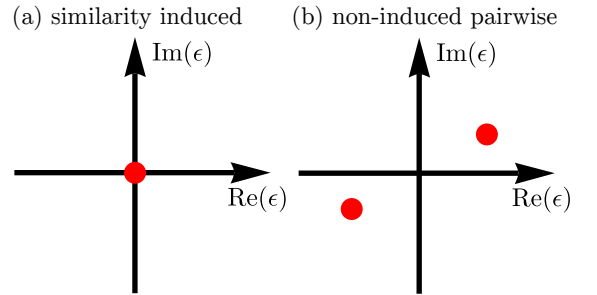


Figure 4. Illustration of how self skew-similarity constrains the position of exceptional structures of  $n$ -band systems (red dots) in the complex eigenvalue plane. (a) Similarity-induced EPs are, when  $m < n$ , forced to appear at the origin, and have codimension  $2k$  when  $m = 2k + \delta$ , where  $\delta = 0$  ( $\delta = 1$ ) for  $n \in \text{even}$  ( $n \in \text{odd}$ ). (b) Despite the similarity, EPs of generic codimension  $2m - 2$  may still appear in the spectrum when  $m < \frac{n}{2}$ , but they are constrained to appear pairwise in adjacent quadrants of the complex eigenvalue plane.

and located at  $\lambda = 0$ . Thus, the EP4s are promoted to EP5s. Since the surfaces of EP2s appear at both finite and zero  $\lambda$ , they are affected differently upon adding the flat band. The EP2 surface at  $\nu = 0$  becomes a 2D surface of EP2s embedded in 4D, while the EP2 surface at  $\nu = \eta^2$  becomes a 2D surface of EP3s.

#### D. Dimensional generalization

Just as for the pseudo-Hermitian systems treated in Sec. III, the exceptional structures induced by self-similarity will be accompanied by generic exceptional structures. The emergence of the generic exceptional structures can be argued for by studying a model given by

$$H = \begin{pmatrix} \mathcal{H} & 0 \\ 0 & -\mathcal{H} \end{pmatrix}. \quad (32)$$



Since this model has a self skew-similar spectrum, it is self skew-similar with respect to some generator. Here,  $H$  is taken to be  $n \times n$  with  $n \in \text{even}$ . Since  $\mathcal{H}$  is a completely generic non-Hermitian operator, the corresponding exceptional structures will be generic, which means that EPms with  $m \leq n/2$  are of codimension  $2m - 2$ . This means that the similarity-induced EPks of codimensions  $k$  (recalling that  $H$  models a system with an even number of bands) are accompanied by generic EPms of codimension  $2m - 2$ . Fig. 4 illustrates that these are further constrained to appear at zero eigenvalue, or pairwise in adjacent quadrants of the complex eigenvalue plane, respectively, to ensure that the similarity-induced spectral constraints hold.

Upon adding a band to  $H$ , which by the similarity is forced to be flat appearing at  $\lambda = 0$ , the similarity-induced EPks will be of codimensions  $k-1$ , and all exceptional degeneracies appearing at  $\lambda = 0$  will be increased by one. Apart from that, the same reasoning as for an even number of bands holds.

This concludes the analysis of self skew-similar systems from the point of view of multifold exceptional structures. In the following section, we apply similar methods to study EPns induced by multiple similarities.

## V. MULTIPLE-SIMILARITIES-INDUCED EXCEPTIONAL STRUCTURES

Imposing multiple similarities simultaneously on the system reduces the codimension of exceptional structures further than what any individual similarity achieves. The combinations of any two different similarities yields identical overall spectral symmetries, namely  $\{\lambda\} = \{\lambda^*\}$ ,  $\{\lambda\} = \{-\lambda^*\}$ , and  $\{\lambda\} = \{-\lambda\}$ . The consequences of this highly symmetric situation are presented in this section.

### A. Implication of triple-similarity and likeness of $2n$ - and $2n + 1$ -band models

An important observation is that any possible pair of two similarities always implies the presence of the third as any combination of two of the spectral symmetries results in the third. Hence, every system with multiple similarities is at least locally self skew-similar everywhere, and we again find the likeness of  $2n$ - and  $2n + 1$ -band systems with the  $(2n + 1)$ th band being completely flat. The degeneracy of all exceptional structures at  $\lambda = 0$  found in  $2n$ -band systems subject to multiple similarities is increased by one upon adding the  $(2n + 1)$ th band, while exceptional structures away from the origin remain unchanged. This allows us to derive all exceptional structure in  $2n$ - and  $2n + 1$ -band systems simultaneously.

The necessary presence of self skew-similarity further allows us to reduce the degree of the characteristic polynomial of a model subject to multiple similarities. A

$2n$ -band model  $H_{2n}$  hosting multiple similarities has a characteristic polynomial on the form

$$P_{2n}(\lambda) = \left( \lambda^{2n} - \sum_{j=0}^{n-1} a_{2j} \lambda^{2j} \right), \quad (33)$$

with  $a_{2j}$  being real valued functions of some parameter space. Using the substitution

$$z = \lambda^2 - \frac{a_{2n-2}}{n} \quad (34)$$

the characteristic polynomial can be transformed to

$$\tilde{P}_n(z) = z^n - \sum_{j=0}^{n-2} b_j z^j, \quad (35)$$

with  $b_j = b_j(a_0, \dots, a_{2n-2}) \in \mathbb{R}$ . Given the  $n$  solutions  $z_l$ , the eigenvalue of  $H_{2n}$  takes the form

$$\lambda_{\pm}(z_l) = \pm \sqrt{z_l + a_{2n-2}/n}. \quad (36)$$

Consequently, multiple-similarities-induced EP $2ns$  are of codimension  $n$ .

### B. Exceptional structures induced by multiple similarities in three dimensions

Using the method above, we will now investigate what exceptional structures are induced by multiple similarities in three dimensions, thus turning to a 6-band model  $H$  and define

$$\kappa = -\frac{\text{tr}(H^2)}{6}, \quad (37)$$

$$\eta = \frac{1}{72} \left\{ [\text{tr}(H^2)]^2 - 6 \text{tr}(H^4) \right\}, \quad (38)$$

$$\nu = -\frac{5 [\text{tr}(H^2)]^3}{864} + \frac{\text{tr}(H^2) \text{tr}(H^4)}{48} - \frac{\det(H)}{2}. \quad (39)$$

The similarities lead to  $\kappa, \eta, \nu \in \mathbb{R}$  in terms of which the characteristic polynomial is given by

$$\mathcal{P}_6(\lambda) = \lambda^6 + 3\kappa\lambda^4 + 3(\eta + \kappa^2)\lambda^2 + (\kappa^3 + 3\kappa\eta - 2\nu). \quad (40)$$

The discriminant reads

$$\mathcal{D}_6 = -746496 (\eta^3 + \nu^2)^2 (\kappa^3 + 3\eta\kappa - 2\nu). \quad (41)$$

Employing the previously introduced mapping  $\lambda = \pm \sqrt{z - \kappa}$  results in the reduced real polynomial

$$\tilde{\mathcal{P}}_6(z) = z^3 + 3\eta z - 2\nu. \quad (42)$$

Solving  $\tilde{\mathcal{P}}_6 = 0$  for  $z$ , the exceptional structure of  $H$  can be derived. With  $\alpha_{\pm} = (\nu \pm \sqrt{\eta^3 + \nu^2})^{1/3}$ ,  $\beta = (1 + i\sqrt{3})/2 = \exp(i\pi/3)$ , and

$$\begin{aligned} z_1 &= \alpha_+ + \alpha_-, & z_2 &= -\beta^* \alpha_+ - \beta \alpha_-, \\ z_3 &= -\beta \alpha_+ - \beta^* \alpha_-, \end{aligned} \quad (43)$$

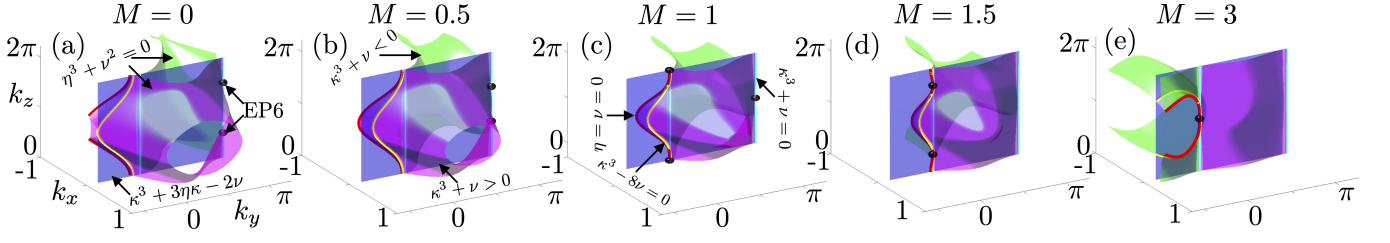


Figure 5. Exceptional structures in part of the Brillouin zone of the model given by Eqs. (45)-(47). As predicted, the EP6s (black dots) are connected by various exceptional structures. The blue surface denote EP2s corresponding to  $\kappa^3 + 3\eta\kappa - 2\nu = 0$ , while the green (purple) surface are EP2s corresponding to  $\eta^3 + \nu^2 = 0$  for  $\kappa^3 + \nu < 0$  ( $\kappa^3 + \nu > 0$ ). On these surfaces are special EP2 arcs, one of which is located at  $\lambda = 0$ , defined by the additional constraint  $\kappa^3 - 8\nu$  (yellow arcs). Along these arcs, all eigenvalues are twofold degenerate. Additionally, if instead  $\kappa^3 + \nu = 0$  on the EP2 surfaces, arcs of EP4s at  $\lambda = 0$  appear (cyan arcs). When  $\eta = \nu = 0$  arcs of either purely real or complex conjugated EP3s emerge (red arcs). All of these structures are possibly connected to EP6s, but as the figure shows, they are not always. For  $M = 0, 0.5$  [panel (a) and (b), respectively], the EP4 arcs connect the EP6s, while the EP3 and special EP2 arcs do not. When this EP6 pair is annihilated at  $M = 1$  [panel (c)], another pair is created. These EP6s are connected by all different EP arcs, see panel (d) for  $M = 1.5$ . At  $M = 3$ , these EP6s are annihilated, resulting in the EP arcs to disconnect.

the six eigenvalues are given by

$$\lambda_{j,\pm} = \pm \sqrt{z_j - \kappa}, \quad (44)$$

where  $j = 1, 2, 3$ .

The similarity-induced EP6s emerge as pairs if the constraints  $\kappa = \eta = \nu = 0$  are met. There are multiple features in the exceptional structure connecting an EP6 pair:

- (i) Arcs along which pairs of EP3s emerge, which are either purely real or imaginary;
- (ii) Surfaces with pairs of real or imaginary EP2s;
- (iii) Arcs of EP4s at  $\lambda = 0$ , which mark one type of intersection between the different EP2 surfaces;
- (iv) Arcs on which there are three distinct eigenvalues, which are all twofold degenerate. These arcs appear on all intersections of different EP2 surfaces, that do not result in an EP4 arcs;
- (v) Surfaces with a single isolated EP2 at  $\lambda = 0$ .

No other exceptional structures can emerge in 6-band systems in the presence of multiple similarities. Although EP5s have codimension 2 in presence of multiple similarities [c.f. Table II], and thus are expected to appear as 1D arcs in a 3D parameter space, the spectral symmetry prevents the EP5s from emerging in a 6-band system, [c.f. Table I].

Let us explain how these structures arise in more detail in the following. First we consider  $\eta = 0$  and  $\nu = 0$  with  $\kappa \neq 0$ . These constraints define two arcs in the 3D parameter space on which EP3s emerge (i). The arcs connect the EP6 pair and the sign of  $\kappa$  determines whether the EP3s are real or imaginary. Similarly to the isolated EP2 arcs in pseudo-Hermitian 4-band systems [cf. Sec. III and the yellow arcs in Figs. 1(a)-(e)], the EP3 arcs here have a codimension different than expected,

the reason being that the EP3s are not induced by both similarities. If the EP3s are real they are induced by the spectral constraint  $\{\lambda\} = \{\lambda^*\}$  while the second spectral constraint  $\{\lambda\} = \{-\lambda^*\}$  or  $\{\lambda\} = \{-\lambda\}$  results in the symmetric appearance of the EP3 arcs. The single spectral constraint reduces the codimension only to 2, and not to 1, and thus the EP3s appear as arcs. For the imaginary EP3s  $\{\lambda\} = \{-\lambda^*\}$  induces the EP3s and the pairwise appearance fulfills the other constraints, which results in codimension 2 for these EP3s as well.

If  $\eta^3 + \nu^2 = 0$  with  $\eta \neq 0 \neq \nu$  we find pairs of EP2 surfaces (ii). For  $-\nu > \kappa^3$  the EP2 pairs are on the real axis, and we find an imaginary pair of EP2s if  $-\nu < \kappa^3$ . In general the remaining eigenvalues are non-degenerate, real for  $8\nu > \kappa$  and imaginary for  $8\nu < \kappa$ .

There are two additional constraints we have to take into account for the  $\eta^3 + \nu^2 = 0$  surface:  $\kappa^3 - 8\nu = 0$  and  $\kappa^3 + \nu = 0$ . If  $\kappa^3 - 8\nu = 0$  there is an additional EP2 at  $\lambda = 0$ , where  $z_i - \kappa = 0$ . This defines an arc in the 3D parameter space on which each eigenvalue is twofold degenerate (iii). When instead  $\kappa^3 + \nu = 0$ , the surface pair of EP2s merge into a single EP4 at the origin of the complex eigenvalue plane (iv). This arc connects pairs of EP6s, and marks the seam between the surface with real and imaginary EP2 pairs.

If the second factor in the discriminant vanishes,  $\kappa^3 + 3\eta\kappa - 2\nu = 0$ , we always find a degeneracy at  $\lambda = 0$  fulfilling  $z_i - \kappa = 0$  for one of the  $z_i$ . This defines another surface of EP2s on which the remaining eigenvalues can be real, imaginary or complex (v). If  $\eta^3 + \nu^2 \neq 0$  the remaining eigenvalues must be non-degenerate. If the  $\kappa^3 + 3\eta\kappa - 2\nu = 0$  surface intersects with the  $\eta^3 + \nu^2 = 0$  surface, we find the  $\kappa^3 - 8\nu = 0$  and  $\kappa^3 + \nu = 0$  arcs discussed before.

Overall we find that similarity-induced EP6 pairs are connected by multiple EP2 surfaces, on which there are two EP3 arcs and two EP4 arcs. 6-band systems with multiple similarities do not host any further exceptional structures. There are however notable Fermi structures

discussed in Appendix B. Due to the high spectral symmetry the number of nontrivial Fermi structures is low for multiple similarity constrained models.

### C. An example

To illustrate the exceptional structures induced by multiple similarities in 3D, we study the model given by

$$H_6 = \begin{pmatrix} 0 & 1 & 0 & 0 & 0 & 0 \\ 0 & 0 & 1 & 0 & 0 & 0 \\ 0 & 0 & 0 & 1 & 0 & 0 \\ 0 & 0 & 0 & 0 & 1 & 0 \\ 0 & 0 & 0 & 0 & 0 & 1 \\ a_0 & 0 & a_2 & 0 & a_4 & 0 \end{pmatrix}, \quad (45)$$

$$a_0 = \sin(k_x), \quad a_2 = \sin(k_y), \quad (46)$$

$$a_4 = M - \cos(k_x) - \cos(k_y) + \cos(k_z), \quad (47)$$

with  $k_x, k_y, k_z$  the lattice momentum components, and  $M \in \mathbb{R}$ . The corresponding exceptional structures are displayed in Fig. 5, and confirm the aforementioned general statements. The pairwise creation/annihilation of the EP6s as a function of the parameter  $M$ , which is swept through in Fig. 5(a)-(e), suggests that these are topological, a topic that we discuss in the following subsection.

Finally, we comment on how these exceptional structures are affected upon adding a seventh band, which due to the similarities necessarily is flat and appear at  $\lambda = 0$ . As mentioned earlier, this promotes all degeneracies appearing at  $\lambda = 0$  by one, while the degeneracies of those appearing at finite  $\lambda$  remain the same. Thus, the degeneracies of the surfaces of EP2s and the arcs of EP3s remain the same at  $\lambda \neq 0$ , while the EP6s, the arcs of EP4s, and the surfaces of EP2s at  $\lambda = 0$  are promoted to EP7s, EP5s, and EP3s, respectively. The special arc, along which all eigenvalues are twofold degenerate, illustrated by a yellow arc in Fig. 5, keeps the pair of nonzero twofold degenerate eigenvalues, and the eigenvalue at  $\lambda = 0$  is promoted to a threefold degeneracy.

### D. Dimensional generalization

Just as for pseudo-Hermiticity and self skew-similarity, systems subject to multiple similarities not only host the exceptional structures induced by multiple similarities, but other structures emerge in the spectrum as well. To illustrate how these emerge, we resort to similar methods as used in previous sections, keeping in mind that this case is slightly more subtle. The spectral constraints imposed by multiple similarities are fulfilled by the following three different operators

$$H_1 = \begin{pmatrix} \mathcal{H}_{\text{PsH}} & 0 \\ 0 & -\mathcal{H}_{\text{PsH}} \end{pmatrix}, \quad (48)$$

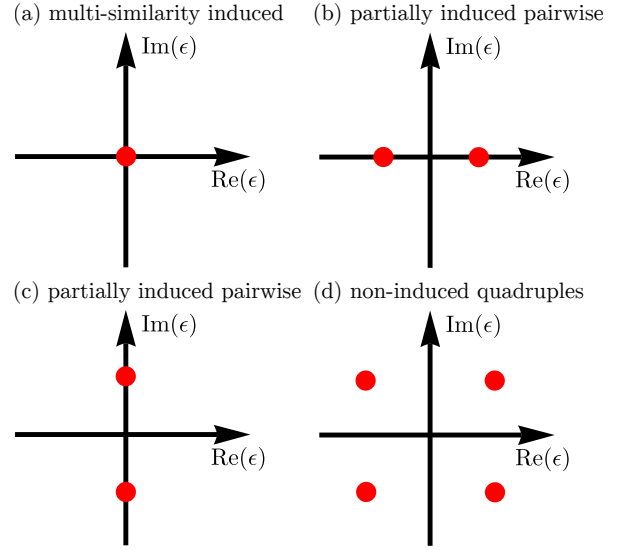


Figure 6. Illustration of how multiple similarities constrain the position of exceptional structures of  $n$ -band systems (red dots) in the complex eigenvalue plane. (a) EPms induced by multiple similarities are forced to appear at the origin, and have codimension  $k$  when  $m = 2k + \delta$  ( $\delta = 0(1)$  for  $m \in \text{even(odd)}$ ). When the EPm is induced only by one similarity relation, its location in the complex eigenvalue plane is bound to satisfy the spectral relation following the remaining similarity. EPms of codimension  $m - 1$  induced only by pseudo-Hermiticity [panel (b)] or self skew-similarity [panel (c)] can emerge when  $m < \frac{n}{2}$ , and are bound to appear at purely real or imaginary eigenvalues of opposite signs, respectively. (d) When  $m < \frac{n}{4}$ , EPms of generic codimension  $2m - 2$  can emerge, and these necessarily appear in all four quadrants.

$$H_2 = \begin{pmatrix} \mathcal{H}_{\text{SSS}} & 0 \\ 0 & \mathcal{H}_{\text{SSS}}^\dagger \end{pmatrix}, \quad (49)$$

$$H_3 = \begin{pmatrix} \mathcal{H} & 0 & 0 & 0 \\ 0 & \mathcal{H}^\dagger & 0 & 0 \\ 0 & 0 & -\mathcal{H} & 0 \\ 0 & 0 & 0 & -\mathcal{H}^\dagger \end{pmatrix}, \quad (50)$$

with  $\mathcal{H}_{\text{PsH}}$  and  $\mathcal{H}_{\text{SSS}}$  being pseudo-Hermitian and self skew-similar  $n/2$ -band models, respectively, and  $\mathcal{H}$  is a generic non-Hermitian operator with  $n/4$  bands. Hence,  $H_1$ ,  $H_2$ , and  $H_3$  describe  $n$ -band models. The form of  $H_1$  indicates that the multiple similarity-induced exceptional structures are accompanied by codimension  $m - 1$  EPms induced by pseudo-Hermiticity only, while the form of  $H_2$  further suggests the existence of self skew-similarity induced EPms of codimension  $m$ , where  $m \leq n/2$  in both cases. Because of the self skew-similarity, the pseudo-Hermiticity-induced EPms necessarily appear in pairs in adjacent quadrants of the complex eigenvalue plane, while the pseudo-Hermiticity enforces the self skew-similarity-induced EPms to appear at purely real eigenvalues, or in pairs at complex conjugate eigenvalues. Lastly, the form of  $H_3$  shows that operators subject to multiple similarities may also host generic EPms of codi-

mension  $2m-2$ . Although the form of  $H_3$  is, in principle, covered as a special case of  $H_1$  and  $H_2$ , writing it out explicitly makes it clear that the EPs of generic codimension display a double mirror symmetry in the complex eigenvalue plane, as they necessarily appear in all four quadrants of the complex plane. The one exception to this is when the exceptional structures appear at the real (imaginary) eigenvalue axis, resulting in a pairwise appearance at some eigenvalue  $\lambda = \pm E_0 \in \mathbb{R}$  ( $\in i\mathbb{R}$ ). This is because of the respective spectral constraint; pseudo-Hermiticity (pseudo anti-Hermiticity) induces a symmetry with respect to the real (imaginary) axis, while self skew-similarity induces a symmetry with respect to the arcs  $\text{Re}(\lambda) = +(-)\text{Im}(\lambda)$  if the signs of the real and imaginary parts of  $\lambda$  are equal (opposite). How the emergence of the different exceptional structures are constrained in the complex eigenvalue plane is displayed in Fig. 6.

Upon adding an additional band to  $H_1$ ,  $H_2$  or  $H_3$ , this is by the similarities enforced to be flat and located at  $\lambda = 0$ . Thus, all exceptional degeneracies appearing at zero eigenvalue will be increased by one. The addition of two bands for  $H_1$  or  $H_2$  increases the dimension of  $\mathcal{H}$  by one. As for  $H_3$ , the case is slightly more subtle, as adding two additional bands reduces the model to either  $H_1$  or  $H_2$ . Only by adding four additional bands, the structure of  $H_3$  can be preserved.

This comprise all possible combinations of exceptional structures in systems subject to multiple similarities. To complement the 3D example of the previous subsection, we in Appendix C present the technical details of the 4D case.

### E. Topological classification of multiple-similarity induced EPns in $n$ -band systems

As hinted by the above 6-band example in 3D, where the EP6s come in pairs, EPns protected by multiple similarities emerging in  $n$ -band models are *topological*. By extending the classification schemes recently developed in Refs. [36, 37], we show that the Abelian eigenvalue topology of EPns is captured by the resultant winding number. We also map out the vector bundle classification and identify the source to the eigenvalue topology in terms of Clifford bundles.

#### 1. Resultant vector and winding number

The resultant winding number is the winding of the resultant vector, in which different resultants of the characteristic polynomial and its corresponding derivatives are collected. For a system subject to multiple similarities, the resultant components from a characteristic polynomial on the form Eq. (33) are defined as

$$r_j = \text{Res} \left[ \partial_\lambda^{n-2j} P_n(\lambda), \partial_\lambda^{n-1} P_n(\lambda) \right], \quad (51)$$

with  $j \in \{1, \dots, \lfloor \frac{n}{2} \rfloor\}$ , where  $\lfloor x \rfloor$  is the floor function and hence denotes the integer part of  $x$ . The resultant vector then reads,

$$\mathbf{R} = (r_1, \dots, r_{\lfloor \frac{n}{2} \rfloor}). \quad (52)$$

Importantly, the resultant vector  $\mathbf{R}$  is constructed in such a way that it vanishes exactly at (and only at) the points in momentum space corresponding to EPns in the parent non-Hermitian Hamiltonian [36, 37]. Therefore, the winding number of the resultant vector around these points can be thought of as “monopole charges” of the EPns. The winding number corresponds to the degree of a map between spheres in the parameter space and the space of resultants,

$$S^{\lfloor \frac{n}{2} \rfloor - 1} \rightarrow S^{\lfloor \frac{n}{2} \rfloor - 1}, \quad (53)$$

$$\frac{\mathbf{k}}{|\mathbf{k}|} \mapsto \frac{\mathbf{R}}{|\mathbf{R}|}, \quad (54)$$

and counts exactly how many times the resultant vector winds around the EPn. As such, this is a topological invariant given by  $\pi_{\lfloor \frac{n}{2} \rfloor - 1}(S^{\lfloor \frac{n}{2} \rfloor - 1}) = \mathbb{Z}$ , when  $n > 3$ , and thus we expect an integer-valued topological invariant classifying these EPns. Up to a normalization factor, the winding number is given by

$$W \propto \oint_{S^{\lfloor \frac{n}{2} \rfloor - 1}} \text{Tr} \left[ (\mathbf{n}^{-1} d\mathbf{n})^{\lfloor \frac{n}{2} \rfloor - 1} \right], \quad (55)$$

with  $\mathbf{n} = \frac{\mathbf{R}}{|\mathbf{R}|}$  the normalized resultant vector. From this winding number follows also a doubling theorem, which can be shown as (using Stokes theorem)

$$\begin{aligned} \sum_k W_k &\propto \sum_k \oint_{S_k^{\lfloor \frac{n}{2} \rfloor - 1}} \text{Tr} \left[ (\mathbf{n}^{-1} d\mathbf{n})^{\lfloor \frac{n}{2} \rfloor - 1} \right] \\ &= \int_{\text{BZ} \setminus \Delta} d\text{Tr} \left\{ [d \log(\mathbf{n})]^{\lfloor \frac{n}{2} \rfloor - 1} \right\} = 0, \end{aligned} \quad (56)$$

where the last step holds using the second Bianchi identity. Here,  $\text{BZ} \setminus \Delta$  denotes the punctured Brillouin zone, i.e., the Brillouin zone with the EPns removed.

Although the above reasoning is in principle applicable also when  $n = 2, 3$ , it is worth commenting on these cases separately. Since  $\pi_0(S^0) = \mathbb{Z}_2$ , we no longer expect an integer invariant classifies two- and threefold EPs induced by multiple similarities. Very much like EP2s induced by pseudo-Hermiticity only (see Ref. [37] for a detailed description), these are instead classified by a  $\mathbb{Z}_2$ -invariant, the origin of which is the introduction of integration on  $S^0$ . Since  $S^0$  comprise a set of two points, integration is defined as a weighted sum of the integrand evaluated at these points. Therefore, the corresponding winding number will take the values  $\pm 1$  always, and the doubling theorem still holds.

#### 2. Resultant Hamiltonian and vector bundle classification

Finally, we unravel the topological nature and origin of the resultant winding number classifying EPns protected



by multiple similarities. The key here lies in the fact that the resultant vector can be used to construct a Hermitian Hamiltonian, known as the resultant Hamiltonian [37],

$$H_{\mathbf{R}}(\mathbf{k}) = \sum_{j=1}^{\lfloor \frac{n}{2} \rfloor} r_j \gamma^j, \quad (57)$$

with  $\gamma^j$  being Clifford algebra generators. By construction, this Hamiltonian hosts nodal points exactly at the same points in momentum space as where the parent non-Hermitian system hosts EP $n$ . As such, the resultant Hamiltonian allows for an interpretation of the non-Hermitian eigenvalue topology in terms of the Hermitian eigenvector topology in the context of the Altland-Zirnbauer symmetry classes [46, 47]. It should be noted that since the spectrum of  $H_{\mathbf{R}}(\mathbf{k})$  is given by  $\pm|\mathbf{R}(\mathbf{k})|$ , the resultant Hamiltonian displays a “generalized spin degeneracy”, as is customary for operators of that form [48].

Which symmetry group determines the topology of these nodal points (and consequently also the corresponding EP $n$ s) is different for different values of  $n$ . When  $\lfloor \frac{n}{2} \rfloor = 2m - 1$  for some integer  $m$ , i.e., when it is odd,  $H_{\mathbf{R}}(\mathbf{k})$  is expressed as a linear combination of all generators of the Clifford algebra of dimension  $2^{\frac{1}{2}(\lfloor \frac{n}{2} \rfloor + 1)} \times 2^{\frac{1}{2}(\lfloor \frac{n}{2} \rfloor + 1)}$ . Hence,  $H_{\mathbf{R}}(\mathbf{k})$  falls within the symmetry class A of the Altland-Zirnbauer classification. The nodal points appear in odd dimensions (since their codimension  $\lfloor \frac{n}{2} \rfloor$  is odd), and are therefore expected to be classified by even-dimensional topological invariants stemming from symmetry class A. These are known to take integer values, and correspond to Chern numbers.

When  $\lfloor \frac{n}{2} \rfloor$  is even, the resultant Hamiltonian lacks one of the  $\gamma$ -matrices in its definition. The remaining  $\gamma$ -matrix can instead be used to define a chiral symmetry, since

$$\{H_{\mathbf{R}}(\mathbf{k}), \gamma^{\lfloor \frac{n}{2} \rfloor + 1}\} = 0. \quad (58)$$

Along the same line of reasoning, the nodal points will in this case be classified by odd-dimensional topological invariants stemming from the AIII symmetry class, which are integer-valued generalized winding numbers.

When  $n = 2, 3$ , the situation is completely different. The resultant Hamiltonian is then a scalar, and does not satisfy chiral symmetry. Most notably is perhaps that EP2s and EP3s induced by multiple similarities thus are not related to Hermitian nodal points through the resultant Hamiltonian, but rather to the zeros of a one-band Hermitian Hamiltonian. This scalar will, however, display other important features when evaluated on the “sphere” surrounding these zeros, since the zero-sphere only comprises two points. Evaluating  $H_{\mathbf{R}}(\mathbf{k})$  on  $S^0$  is done as

$$H_{\mathbf{R}}(k)|_{S^0} = \begin{cases} H_{\mathbf{R}}(-p)\sigma(-p) \\ H_{\mathbf{R}}(p)\sigma(p) \end{cases} = \begin{cases} -H_{\mathbf{R}}(-p) \\ H_{\mathbf{R}}(p) \end{cases}. \quad (59)$$

Bands	$n = 2, 3$	$\lfloor \frac{n}{2} \rfloor$ even	$\lfloor \frac{n}{2} \rfloor$ odd
Inv.	$\mathbb{Z}_2$	$\mathbb{Z}$	$\mathbb{Z}$
Res. Ham.	$H_{\mathbf{R}} = R$	$H_{\mathbf{R}} = \sum_{i=1}^{\lfloor \frac{n}{2} \rfloor} r_i \gamma^i, \{H_{\mathbf{R}}, \gamma^{\lfloor \frac{n}{2} \rfloor + 1}\} = 0$	$H_{\mathbf{R}} = \sum_{i=1}^{\lfloor \frac{n}{2} \rfloor} r_i \gamma^i$
Herm. Deg.	$2^0$	$2^{\frac{1}{2}(\lfloor \frac{n}{2} \rfloor + 1)}$	$2^{\frac{1}{2}(\lfloor \frac{n}{2} \rfloor + 1)}$
Sym. Class	D	AIII	A
Vector Bundle	$TS^1$ , rank 1	$T\mathbb{T}^{\lfloor \frac{n}{2} \rfloor}$ , rank $\lfloor \frac{n}{2} \rfloor$	$T\mathbb{T}^{\lfloor \frac{n}{2} \rfloor}$ , rank $\lfloor \frac{n}{2} \rfloor$
Vector Field	$R \in \Gamma(TS^1)$	$\mathbf{R} \in \Gamma(T\mathbb{T}^{\lfloor \frac{n}{2} \rfloor})$	$\mathbf{R} \in \Gamma(T\mathbb{T}^{\lfloor \frac{n}{2} \rfloor})$

Table III. Summary of the topological nature and origin of the invariants classifying EP $n$ s.

If we now let  $\mathbf{k} \rightarrow -\mathbf{k}$ ,  $H_{\mathbf{R}}(\mathbf{k}) \xrightarrow{\mathbf{k} \rightarrow -\mathbf{k}} -H_{\mathbf{R}}(-\mathbf{k})$ . Thus, the resultant Hamiltonian in this case satisfies a particle-hole symmetry with identity as generator, and therefore falls into symmetry class D. This agrees with the previous observation that the resultant winding number only attains values of  $\pm 1$ . The invariant stemming from symmetry class D is indeed known to be a  $\mathbb{Z}_2$ -invariant.

As a final, somewhat technical, comment regarding the topological origin of the resultant winding number, we also state the vector bundle classification of EP $n$ s induced by multiple similarities. In fact, these can be read off directly from the codimension of the EP $n$ , as listed in Ref. [37]. In general, the correct vector bundle for classifying EP $n$ s is the tangent bundle of  $\mathbb{T}^{\lfloor \frac{n}{2} \rfloor}$ , i.e.,  $T\mathbb{T}^{\lfloor \frac{n}{2} \rfloor}$ , meaning that the resultant vector can be thought of as a vector field on  $\mathbb{T}^{\lfloor \frac{n}{2} \rfloor}$ , since  $\mathbf{R}$  is a section of the tangent bundle denoted  $\mathbf{R} \in \Gamma(T\mathbb{T}^{\lfloor \frac{n}{2} \rfloor})$ . Thus, the resultant vector for EP2s and EP3s is a vector field on the circle  $S^1$ , for EP4s and EP5s it is a vector field on the torus  $\mathbb{T}^2$ , and so on. For technical details behind the vector bundle construction, we refer to Refs. [37, 48]. The contents of this section are summarized in Table III.

## VI. CONCLUDING REMARKS

### A. Summary

In this work, we have mapped out the exceptional structures induced by one and multiple generalized similarities in three and four dimensions. We find that the EP4s induced by pseudo-Hermiticity in three dimensions emerge as special points on similarity-induced arcs of EP3s, which in turn are special arcs on similarity-induced surfaces of EP2s. In addition we find special arcs of EP2s, where the spectral constraints manifest as forcing these to emerge either at purely real eigenvalues, or as pairs of complex conjugate eigenvalues, leading to their differing codimension. Similarly, we find that the EP4s induced

by self skew-similarity in four dimensions are accompanied by different surfaces of EP2s, one located at zero eigenvalue, and one located at a finite eigenvalue. Consequently, these behave differently upon adding a fifth band at zero eigenvalue, promoting the EP4s to EP5s, but only one of the EP2 surfaces to a surface of EP3s.

When exposed to multiple similarities, a system displays an even more exotic plethora of exceptional structures. In three dimensions, the similarity-induced EP6s are found to emerge as special points on similarity-induced arcs of EP4s at zero eigenvalue, which in turn emerge as special arcs on similarity-induced surfaces of EP2s. Additionally, these are accompanied by exceptional structures that are induced by only one of the similarities, giving paired arcs of EP3s emerging at purely real or imaginary eigenvalue, arcs of EP2s where three distinct eigenvalues are twofold degenerate, and a single surface of EP2s at zero eigenvalue. Notably, the spectral constraints do not allow EP5s to appear in this setting. When adding a seventh flat band, the exceptional degeneracies appearing at zero eigenvalue are increased by one.

Our specific studies also allow us to make statements in an arbitrary number of dimensions. We are led to conclude that pseudo-Hermitian systems in addition to similarity-induced codimension  $k - 1$  manifolds of EP $k$ s, also host generic codimension  $2(l - 1)$  manifolds of EP $l$ s, on which the spectral symmetries are reflected as enforcing these to either real eigenvalues, or that they emerge as pairs of complex conjugate eigenvalues (cf. Fig. 2). Similarly, in self skew-similar systems, the similarity-induced EP $k$ s of codimension  $\lfloor k \rfloor$  are accompanied by generic codimension  $2(l - 1)$  manifolds of EP $l$ s, where the spectral symmetries determine the location in the complex eigenvalue planes of the EP $l$ s [cf. Fig. 4]. Along an identical line of reasoning, the codimension  $\lfloor \frac{k}{2} \rfloor$  EP $k$ s induced by multiple similarities are accompanied by exceptional structures of EP $l$ s induced by pseudo-Hermiticity (codimension  $l - 1$ ) and self skew-similarity (codimension  $\lfloor l \rfloor$ ) alone, and generic EP $j$ s (codimension  $2(j - 1)$ ), where the combined similarities constrain their emergence in the complex eigenvalue plane, as illustrated in Fig. 6. Lastly, we provide a classification of the Abelian eigenvalue topology of EP $n$ s induced by multiple similarities in  $n$ -band systems using the resultant winding number.

## B. Discussion and outlook

Apart of providing a missing piece of forefront theoretical research within non-Hermitian topological band theory and providing a complete insight of the emergence of similarity-induced exceptional structures in arbitrary dimensions, our work is of experimental relevance in several modern physical platforms. Starting with the cases of single similarities,  $\mathcal{PT}$ -symmetric systems are an important special case following the studies of pseudo-Hermitian similarity [34]. In optics,  $\mathcal{PT}$

symmetry manifests as a perfect balance between gain and loss in photonic crystals [2–4], where our work can be used to increase the fundamental understanding of systems with three or more variable system parameters. Moreover,  $\mathcal{PT}$ -symmetric systems can also be constructed using electrical circuits, where the corresponding Laplacian reflects the symmetry if resistivity is introduced in a balanced way [49]. Thus, topoelectrical circuits comprise a suggestive class of systems, where parts of our theoretical predictions could be experimentally probed. Other promising candidates include single photon-interferometry, where symmetry-protected rings of EP2s [29], and EP3s [39] have been demonstrated, spin-orbit-coupled cold atoms, where EP3s are found [40], coupled acoustic cavities hosting arcs of EP3s on EP2 surfaces [50], nitrogen-vacancy spin systems, so far realizing arcs of EP3s [51], and correlated quantum many-body systems, where EP4s induced by symmetry-preserving interactions have been theoretically predicted in three spatial dimensions [52]. Moving to self skew-similarity, it comprises a generalization of the physically important sublattice symmetry, commonly present in non-Hermitian Lieb lattices [53–55], yet another important non-Hermitian extension of optics.

Concerning systems subject to multiple similarities, a very recent work suggest that Kerr ring resonators serve as a viable experimental platform [56]. Although present progress is limited to a 2D parameter space, a 3D generalization of such a setup is a good candidate to realize the features predicted in Sec. V well within experimental reach.

Apart from experimental relevance and potential future experimental advances, there are additional theoretical directions to investigate further. One such example is to combine the local similarities studied in this work, with non-local versions, including non-Hermitian time-reversal symmetries, particle-hole symmetries and inversion symmetry [22]. The Abelian eigenvalue topology of EP $n$ s induced by these symmetries were recently classified in terms of the Hermitian tenfold way [46, 47, 57, 58], utilizing a mapping between non-Hermitian eigenvalue topology and Hermitian eigenvector topology [37]. Although not reducing the codimension of the EPs [22], these symmetries drastically change the topological properties of EP $n$ s in  $n$ -band systems when no other similarities/symmetries are present [37], and suggestively they should do the same for the less degenerate exceptional structures on which these EP $n$ s reside. Also, it is not understood if these symmetries further constrain EP $m$ s,  $m < n$ , to only emerge in certain regions of the complex eigenvalue plane, which opens up possibilities for further studies along these lines.

Conclusively, our work not only provides a missing piece of modern research within theoretical non-Hermitian physics, but also displays how abstract mathematical notions could manifest in realistic laboratory setups thanks to its direct relevance in a large variety of areas in modern experimental physics. Having a funda-

mental understanding of the spectral properties provide a powerful and versatile tool for predicting exotic, novel and potentially hitherto unknown phenomena. Therefore, developing this framework further and deepening the connection between mathematics and physics comprises an important and natural step in expanding the vast subject of topological band theory.

## ACKNOWLEDGMENTS

M.S. thanks Lukas König and Lukas Rødland for stimulating discussions and related collaborations. A.M. and F.K.K. acknowledge funding from the Max Planck So-

cietät Lise Meitner Excellence Program 2.0. A.M. and F.K.K. also acknowledge funding from the European Union via the ERC Starting Grant “NTopQuant”. Views and opinions expressed are however those of the authors only and do not necessarily reflect those of the European Union or the European Research Council (ERC). Neither the European Union nor the granting authority can be held responsible for them. M.S. is supported by the Swedish Research Council (VR) under grant NO. 2024-00272. J.I. thanks the Max Planck-uOttawa Centre for Extreme and Quantum Photonics for funding the MPC Internship at the MPI for the Science of Light in Erlangen.

- 
- [1] E. J. Bergholtz, J. C. Budich, and F. K. Kunst, Exceptional topology of non-hermitian systems, *Rev. Mod. Phys.* **93**, 015005 (2021).
  - [2] Ş. K. Özdemir, S. Rotter, F. Nori, and L. Yang, Parity-time symmetry and exceptional points in photonics, *Nature materials* **18**, 783 (2019).
  - [3] L. Lu, J. D. Joannopoulos, and M. Soljačić, Topological photonics, *Nature Photonics* **8**, 821 (2014).
  - [4] T. Ozawa, H. M. Price, A. Amo, N. Goldman, M. Hafezi, L. Lu, M. C. Rechtsman, D. Schuster, J. Simon, O. Zilberberg, and I. Carusotto, Topological photonics, *Rev. Mod. Phys.* **91**, 015006 (2019).
  - [5] S. Khandelwal, N. Brunner, and G. Haack, Signatures of liouvillian exceptional points in a quantum thermal machine, *PRX Quantum* **2**, 040346 (2021).
  - [6] N. Hatano, Exceptional points of the lindblad operator of a two-level system, *Molecular Physics* **117**, 2121 (2019).
  - [7] G. Lindblad, On the generators of quantum dynamical semigroups, *Communications in Mathematical Physics* **48**, 119 (1976).
  - [8] M. Kreibich, J. Main, H. Cartarius, and G. Wunner, Realizing  $\mathcal{PT}$ -symmetric non-hermiticity with ultracold atoms and hermitian multiwell potentials, *Phys. Rev. A* **90**, 033630 (2014).
  - [9] A. Ghatak, M. Brandenbourger, J. van Wezel, and C. Couais, Observation of non-hermitian topology and its bulk-edge correspondence in an active mechanical metamaterial, *Proceedings of the National Academy of Sciences* **117**, 29561 (2020).
  - [10] J. Schindler, Z. Lin, J. M. Lee, H. Ramezani, F. M. Ellis, and T. Kottos,  $\mathcal{PT}$ -symmetric electronics, *Journal of Physics A: Mathematical and Theoretical* **45**, 444029 (2012).
  - [11] X. Yang, J. Li, Y. Ding, M. Xu, X.-F. Zhu, and J. Zhu, Observation of transient parity-time symmetry in electronic systems, *Phys. Rev. Lett.* **128**, 065701 (2022).
  - [12] F. Yang, Q.-D. Jiang, and E. J. Bergholtz, Liouvillian skin effect in an exactly solvable model, *Phys. Rev. Res.* **4**, 023160 (2022).
  - [13] F. K. Kunst, E. Edvardsson, J. C. Budich, and E. J. Bergholtz, Biorthogonal bulk-boundary correspondence in non-hermitian systems, *Phys. Rev. Lett.* **121**, 026808 (2018).
  - [14] S. Yao and Z. Wang, Edge states and topological invariants of non-hermitian systems, *Phys. Rev. Lett.* **121**, 086803 (2018).
  - [15] E. Edvardsson, F. K. Kunst, and E. J. Bergholtz, Non-hermitian extensions of higher-order topological phases and their biorthogonal bulk-boundary correspondence, *Phys. Rev. B* **99**, 081302 (2019).
  - [16] J. T. Gohsrich, A. Banerjee, and F. K. Kunst, The non-hermitian skin effect: A perspective, *Europhysics Letters* (2025).
  - [17] T. Kato, *Perturbation theory of linear operators*, edited by A. Cappelli and G. Mussardo (Springer, Berlin, 1966).
  - [18] W. D. Heiss, The physics of exceptional points, *Journal of Physics A: Mathematical and Theoretical* **45**, 444016 (2012).
  - [19] I. Rotter, A non-hermitian hamilton operator and the physics of open quantum systems, *Journal of Physics A: Mathematical and Theoretical* **42**, 153001 (2009).
  - [20] M. V. Berry, Physics of nonhermitian degeneracies, *Czechoslovak journal of physics* **54**, 1039 (2004).
  - [21] P. Delplace, T. Yoshida, and Y. Hatsugai, Symmetry-protected multifold exceptional points and their topological characterization, *Phys. Rev. Lett.* **127**, 186602 (2021).
  - [22] S. Sayyad and F. K. Kunst, Realizing exceptional points of any order in the presence of symmetry, *Phys. Rev. Res.* **4**, 023130 (2022).
  - [23] J. Carlström and E. J. Bergholtz, Exceptional links and twisted fermi ribbons in non-hermitian systems, *Phys. Rev. A* **98**, 042114 (2018).
  - [24] R. A. Molina and J. González, Surface and 3d quantum hall effects from engineering of exceptional points in nodal-line semimetals, *Phys. Rev. Lett.* **120**, 146601 (2018).
  - [25] K. Moors, A. A. Zyuzin, A. Y. Zyuzin, R. P. Tiwari, and T. L. Schmidt, Disorder-driven exceptional lines and fermi ribbons in tilted nodal-line semimetals, *Phys. Rev. B* **99**, 041116 (2019).
  - [26] J. Carlström, M. Stålhammar, J. C. Budich, and E. J. Bergholtz, Knotted non-hermitian metals, *Phys. Rev. B* **99**, 161115 (2019).
  - [27] X. Zhang, G. Li, Y. Liu, T. Tai, R. Thomale, and C. H. Lee, Tidal surface states as fingerprints of non-hermitian nodal knot metals, *Communications Physics* **4**, 47 (2021).

- [28] M. Stålhammar, L. Rødland, G. Arone, J. C. Budich, and E. J. Bergholtz, Hyperbolic nodal band structures and knot invariants, *SciPost Phys.* **7**, 019 (2019).
- [29] K. Wang, L. Xiao, J. C. Budich, W. Yi, and P. Xue, Simulating exceptional non-hermitian metals with single-photon interferometry, *Phys. Rev. Lett.* **127**, 026404 (2021).
- [30] J. C. Budich, J. Carlström, F. K. Kunst, and E. J. Bergholtz, Symmetry-protected nodal phases in non-hermitian systems, *Phys. Rev. B* **99**, 041406(R) (2019).
- [31] S. Sayyad, M. Stålhammar, L. Rødland, and F. K. Kunst, Symmetry-protected exceptional and nodal points in non-Hermitian systems, *SciPost Phys.* **15**, 200 (2023).
- [32] I. Mandal and E. J. Bergholtz, Symmetry and higher-order exceptional points, *Phys. Rev. Lett.* **127**, 186601 (2021).
- [33] M. Stålhammar and E. J. Bergholtz, Classification of exceptional nodal topologies protected by  $\mathcal{PT}$  symmetry, *Phys. Rev. B* **104**, L201104 (2021).
- [34] A. Montag and F. K. Kunst, Essential implications of similarities in non-hermitian systems, *Journal of Mathematical Physics* **65** (2024).
- [35] A. Montag and F. K. Kunst, Symmetry-induced higher-order exceptional points in two dimensions, *Phys. Rev. Res.* **6**, 023205 (2024).
- [36] T. Yoshida, J. L. K. König, L. Rødland, E. J. Bergholtz, and M. Stålhammar, Winding topology of multifold exceptional points, *Phys. Rev. Res.* **7**, L012021 (2025).
- [37] M. Stålhammar and L. Rødland, Abelian spectral topology of multifold exceptional points, *arXiv:2412.15323* (2024).
- [38] R. Okugawa and T. Yokoyama, Topological exceptional surfaces in non-hermitian systems with parity-time and parity-particle-hole symmetries, *Phys. Rev. B* **99**, 041202(R) (2019).
- [39] K. Wang, L. Xiao, H. Lin, W. Yi, E. J. Bergholtz, and P. Xue, Experimental simulation of symmetry-protected higher-order exceptional points with single photons, *Science Advances* **9**, eadi0732 (2023).
- [40] Y.-J. Liu, K. K. Pak, P. Ren, M. Guo, E. Zhao, C. He, and G.-B. Jo, Third-order exceptional point in non-hermitian spin-orbit-coupled cold atoms, *arXiv:2412.17705* (2025).
- [41] K. Kawabata, K. Shiozaki, M. Ueda, and M. Sato, Symmetry and topology in non-hermitian physics, *Phys. Rev. X* **9**, 041015 (2019).
- [42] T. L. Curtright, D. B. Fairlie, and H. Alshal, A galileon primer, *arXiv:1212.6972* (2012).
- [43] L. Brand, The companion matrix and its properties, *The American Mathematical Monthly* **71**, 629 (1964).
- [44] V. I. Arnold, On matrices depending on parameters, *Russian Mathematical Surveys* **26**, 29 (1971).
- [45] M. Udagawa and E. J. Bergholtz, Field-selective anomaly and chiral mode reversal in type-II weyl materials, *Phys. Rev. Lett.* **117**, 086401 (2016).
- [46] A. Altland and M. R. Zirnbauer, Nonstandard symmetry classes in mesoscopic normal-superconducting hybrid structures, *Phys. Rev. B* **55**, 1142 (1997).
- [47] S. Ryu, A. P. Schnyder, A. Furusaki, and A. W. W. Ludwig, Topological insulators and superconductors: tenfold way and dimensional hierarchy, *New Journal of Physics* **12**, 065010 (2010).
- [48] V. Mathai and G. C. Thiang, Differential topology of semimetals, *Communications in Mathematical Physics* **355**, 561 (2017).
- [49] N. K. Gupta and A. M. Jayannavar, Non-hermitian topoelectrical circuits: Expedient tools for topological state engineering with gain-loss modulation, *arXiv:2108.11587* (2021).
- [50] W. Tang, K. Ding, and G. Ma, Realization and topological properties of third-order exceptional lines embedded in exceptional surfaces, *Nature Communications* **14**, 6660 (2023).
- [51] Y. Wu, Y. Wang, X. Ye, W. Liu, Z. Niu, C.-K. Duan, Y. Wang, X. Rong, and J. Du, Third-order exceptional line in a nitrogen-vacancy spin system, *Nature Nanotechnology* **19**, 160 (2024).
- [52] R. Schäfer, J. C. Budich, and D. J. Luitz, Symmetry protected exceptional points of interacting fermions, *Phys. Rev. Res.* **4**, 033181 (2022).
- [53] R. A. Vicencio, C. Cantillano, L. Morales-Inostroza, B. Real, C. Mejia-Cortés, S. Weimann, A. Szameit, and M. I. Molina, Observation of localized states in lieb photonic lattices, *Phys. Rev. Lett.* **114**, 245503 (2015).
- [54] S. Mukherjee, A. Spracklen, D. Choudhury, N. Goldman, P. Öhberg, E. Andersson, and R. R. Thomson, Observation of a localized flat-band state in a photonic lieb lattice, *Phys. Rev. Lett.* **114**, 245504 (2015).
- [55] Y.-X. Xiao, K. Ding, R.-Y. Zhang, Z. H. Hang, and C. T. Chan, Exceptional points make an astroid in non-hermitian lieb lattice: Evolution and topological protection, *Phys. Rev. B* **102**, 245144 (2020).
- [56] L. Hill, J. T. Gohsrich, A. Ghosh, J. Fauman, P. Del'Haye, and F. K. Kunst, *Exceptional, but separate: Precursors to spontaneous symmetry breaking* (2025), *arXiv:2505.02691 [physics.optics]*.
- [57] A. P. Schnyder, S. Ryu, A. Furusaki, and A. W. W. Ludwig, Classification of topological insulators and superconductors in three spatial dimensions, *Phys. Rev. B* **78**, 195125 (2008).
- [58] A. Kitaev, V. Lebedev, and M. Feigel'man, Periodic table for topological insulators and superconductors, in *AIP Conference Proceedings* (AIP, 2009).
- [59] R. Zhang, H. Qin, and J. Xiao,  $\mathcal{PT}$ -symmetry entails pseudo-hermiticity regardless of diagonalizability, *Journal of Mathematical Physics* **61** (2020).

## Appendix A: Proof of equivalence of the similarity and the spectral symmetry

For a generic finite-dimensional dynamical matrix  $H$  we show in the following that spectral symmetries imply generalized similarities of the matrix. This proves that the generalized similarities and spectral symmetries are equivalent.

**Lemma A.1.** *A matrix  $H \in \mathbb{C}^{n \times n}$  is pseudo-Hermitian if its spectrum fulfills  $\{\lambda\} = \{\lambda^*\}$ .*

*Proof.* The proof is an adaptation of the proof of pseudo-Hermiticity derived in Ref. [59]. We explicitly construct the Hermitian matrix  $\eta$  with  $H = \eta H^\dagger \eta^{-1}$  to prove the lemma. Using its Jordan canonical form  $J$  the matrix  $H$  can be written as

$$H = QJQ^{-1}, \quad (\text{A1})$$



where  $Q$  is an invertible matrix. The Jordan canonical form consists of Jordan blocks that have the form

$$J(\lambda) = \begin{pmatrix} \lambda & 1 & & \\ & \ddots & \ddots & \\ & & \lambda & 1 \\ & & & \lambda \end{pmatrix}_{m \times m}, \quad (\text{A2})$$

where  $m$  is the size of the Jordan block and  $m = 1$  reduces to  $\lambda$ . Given the spectral symmetry  $\{\lambda\} = \{\lambda^*\}$  the eigenvalues are either purely real  $\lambda = a$  or come in pairs of the form  $\lambda = a + ib$  and  $\lambda^* = a - ib$ , where  $a, b \in \mathbb{R}$ . We define two kinds of matrix blocks

$$K_1 = J(a)_{m \times m}, \quad (\text{A3})$$

$$K_2 = \begin{pmatrix} J(a + ib) & 0 \\ 0 & J(a - ib) \end{pmatrix}_{2l \times 2l}, \quad (\text{A4})$$

and express the Jordan canonical form as the block diagonal matrix  $J = \text{diag}(M_1, \dots, M_k)$  with each block  $M_j$  being either of the form  $K_1$  or  $K_2$ . We can prove explicitly that the Jordan form constructed in this ordered form is pseudo-Hermitian. Both types of matrix blocks satisfy  $M_j = G_j M_j^\dagger G_j^{-1}$  with the Hermitian matrix

$$G_j = \begin{pmatrix} 0 & \dots & 0 & 1 \\ \vdots & \ddots & 1 & 0 \\ 0 & \ddots & \ddots & \vdots \\ 1 & 0 & \dots & 0 \end{pmatrix}. \quad (\text{A5})$$

From these  $G_j$  we construct the Hermitian matrix  $G = \text{diag}(G_1, \dots, G_k)$ , and this satisfies

$$J = G J^\dagger G^{-1}, \quad (\text{A6})$$

which shows that the Jordan canonical form is pseudo-Hermitian. We insert this in Eq. (A1) and we obtain

$$\begin{aligned} H &= Q J Q^{-1} \\ &= -Q G J^\dagger G^{-1} Q^{-1} \\ &= -Q G (Q^{-1} H Q)^\dagger G^{-1} Q^{-1} \\ &= -(Q G Q^\dagger) H^\dagger (Q G Q^\dagger)^{-1}. \end{aligned} \quad (\text{A7})$$

Because  $G$  is Hermitian,  $\Gamma = Q G Q^\dagger$  is Hermitian as well. This completes the proof that  $H$  is pseudo-Hermitian.

**Lemma A.2.** A matrix  $H \in \mathbb{C}^{n \times n}$ ,  $H$  is anti pseudo-Hermitian if its spectrum fulfills  $\{\lambda\} = \{-\lambda^*\}$ .

*Proof.* The proof is an adaptation of the proof of pseudo-Hermiticity derived in Ref. [59]. We explicitly construct the Hermitian matrix  $\Gamma$  with  $H = -\Gamma H^\dagger \Gamma^{-1}$  to prove the lemma. Using its Jordan canonical form  $J$  the matrix  $H$  can be written by

$$H = Q J Q^{-1}, \quad (\text{A8})$$

where  $Q$  is an invertible matrix. The Jordan canonical form consists of Jordan blocks that have the form

$$J(\lambda) = \begin{pmatrix} \lambda & 1 & & \\ & \ddots & \ddots & \\ & & \lambda & 1 \\ & & & \lambda \end{pmatrix}_{m \times m}, \quad (\text{A9})$$

where  $m$  is the size of the Jordan block and  $m = 1$  reduces to  $\lambda$ . Given the spectral similarity  $\{\lambda\} = \{-\lambda^*\}$  the eigenvalues are either purely imaginary  $\lambda = ib$  or come in pairs of the form  $\lambda = a + ib$  and  $-\lambda^* = -a + ib$ , where  $a, b \in \mathbb{R}$ . We define two kinds of matrix blocks

$$K_1 = J(ib)_{m \times m}, \quad (\text{A10})$$

$$K_2 = \begin{pmatrix} J(a + ib) & 0 \\ 0 & J(-a + ib) \end{pmatrix}_{2l \times 2l}, \quad (\text{A11})$$

and express the Jordan canonical form as the block diagonal matrix  $J = \text{diag}(M_1, \dots, M_k)$  with each block  $M_j$  being either of the form  $K_1$  or  $K_2$ . We can prove explicitly that the Jordan form constructed in this ordered form is anti pseudo-Hermitian. Both types of matrix blocks satisfy  $M_j = -G_j M_j^\dagger G_j^{-1}$  with the Hermitian matrix

$$G_j = \begin{pmatrix} 0 & \dots & 0 & 1 \\ \vdots & \ddots & 1 & 0 \\ 0 & \ddots & \ddots & \vdots \\ 1 & 0 & \dots & 0 \end{pmatrix}. \quad (\text{A12})$$

From these  $G_j$  we construct the Hermitian matrix  $G = \text{diag}(G_1, \dots, G_k)$ , and this satisfies

$$J = -G J^\dagger G^{-1}, \quad (\text{A13})$$

which shows that the Jordan canonical form is anti pseudo-Hermitian. We insert this in Eq. (A8) and we obtain

$$\begin{aligned} H &= Q J Q^{-1} \\ &= -Q G J^\dagger G^{-1} Q^{-1} \\ &= -Q G (Q^{-1} H Q)^\dagger G^{-1} Q^{-1} \\ &= -(Q G Q^\dagger) H^\dagger (Q G Q^\dagger)^{-1}. \end{aligned} \quad (\text{A14})$$

Because  $G$  is Hermitian,  $\Gamma = Q G Q^\dagger$  is Hermitian as well. This completes the proof that  $H$  is anti pseudo-Hermitian.

**Lemma A.3.** A matrix  $H \in \mathbb{C}^{n \times n}$ ,  $H$  is self skew-similar if its spectrum fulfills  $\{\lambda\} = \{-\lambda\}$ .

*Proof.* The Jordan canonical  $J$  form is given by

$$J = Q_+^{-1} H Q_+. \quad (\text{A15})$$

The rows and columns can be freely rearranged. Due to the spectral symmetry we find  $Q_-$ , such that

$$J = -Q_-^{-1} H Q_-. \quad (\text{A16})$$

The reason for this is that  $H$  and  $-H$  have an identical spectrum. Therefore we can define  $S = Q_+ Q_-^{-1}$  and this results in self skew-similarity

$$H = -SHS^{-1}. \quad (\text{A17})$$

## Appendix B: Multifold Fermi Structures in Similarity Constraint Systems

In addition to exceptional structures, non-Hermitian systems host further topological features known as bulk Fermi structures (as a generalization of the terms *arc* and *surface*). These mark degeneracies in the real or imaginary parts of the eigenvalues only, leaving the eigenvalues themselves non-degenerate. In systems subject to similarities, the simplest Fermi structures (where the real or imaginary parts are two-fold degenerate) are of the same dimension as the parameter space, making them trivial [35]. Similarly we find for higher-band systems similarity-induced Fermi structures with codimension 0. These structures are a trivial result of the spectral symmetry, which is enforced by the similarity and we will not discuss them in detail. Instead we will focus on all Fermi structures that emerge with a codimension greater or equal to 1, which we call non-trivial. In this Appendix systematically map out the non-trivial multifold Fermi structures induced by the different similarity relations [35], treating pseudo-Hermiticity in Appendix B 1, self skew-similarity in Appendix B 2, and multiple similarities in Appendix B 3.

### 1. Multifold Fermi structures induced by pseudo-Hermiticity

There are three non-trivial Fermi structures arising in 4-band pseudo-Hermitian systems:

- (i) 2D 3-level imaginary Fermi surfaces, which terminate on the EP2 surfaces along the EP3 arcs. The eigenvalues along these surfaces are given by  $\lambda_1 = -3x$ ,  $\lambda_2 = x$ ,  $\lambda_3 = x + iy$ ,  $\lambda_4 = x - iy$ . The constraints on the parameters of the characteristic polynomial are given by three non-linear equations, namely  $3\alpha = y^2 - 6x^2$ ,  $\sqrt{2}\beta = 8x^3 + 2xy^2$ , and  $\gamma = -4x^4 - 4x^2y^2$ . These constraints are equivalent to the conditions Eqs. (14) and (15) from the main text. In the main text we present a condition for the Fermi surfaces following Descartes method, while we derive a set of non-linear equations for the coefficients of the characteristic polynomial here. The codimension of the Fermi surface is 1 even though three equations have to be fulfilled, the reason being that we have introduced  $x$  and  $y$  as additional degrees of freedom;
- (ii) 2D surface with a pair of 2-level Fermi surfaces with  $\text{Re}[\lambda] \neq 0$ . The surface is defined by  $\beta = 0$  and

$3\alpha^2 - \gamma < 0$ , and is connected to both the arcs which host a pair of real EP2s and the arcs that hosts purely imaginary EP2s;

- (iii) 2D 4-level imaginary Fermi surface, defined by  $\beta = 0$  and  $0 < \gamma < 3\alpha^2$ . On this Fermi surface all four eigenvalues are purely imaginary and non-degenerate.

The latter two Fermi structures emerge on surfaces in parameter space, on which the pseudo-Hermitian matrix acquires the remaining two similarities locally.

The results in this section can be extended to pseudo anti-Hermitian systems in a straightforward manner: the Fermi structures for a pseudo anti-Hermitian system  $\tilde{H}(\mathbf{k})$  are found by rotating those of a pseudo-Hermitian system  $H' = -i\tilde{H}$  by  $\pi/2$  in the complex plane. This means that any eigenvalue  $\lambda$  of  $H'$  is mapped to  $\tilde{\lambda} = -i\lambda$ , which is an eigenvalue of  $\tilde{H}$ . This shows that any exceptional point in the spectrum of  $\tilde{H}$  can be derived by considering the exceptional structure of  $H'$ . For four-band pseudo anti-Hermitian models in particular this implies the presence of pairs of 2D 3-level Fermi surfaces, pairs of imaginary two-level Fermi surfaces, and 4 level Fermi surfaces..

### 2. Multifold Fermi structures induced by self skew-similarity

In self-skew similar systems non-trivial Fermi structures arise only if the parent dynamical matrix acquires the remaining two similarities locally. This is expressed by the two constraints  $\eta \in \mathbb{R}$  and  $\nu \in \mathbb{R}$ , which define surfaces in the 4D parameter space. The signs of both  $\eta$  and  $\nu$  result in four distinct Fermi structures, all of which are defined on 2D surfaces:

- (i) a pair of a 2-level real and a 2-level imaginary Fermi surface for  $\nu < 0$ ;
- (ii) a 4-level Fermi surface for  $\eta < 0$  and  $\eta^2 > \nu > 0$ ;
- (iii) a 4-level imaginary Fermi surface for  $\eta > 0$  and  $\eta^2 > \nu > 0$ .

There are no further Fermi structures that may emerge due to the spectral symmetry of the self skew-similar matrix.

### 3. Multifold Fermi structures induced by multiple similarities

Systems with multiple similarities are so heavily constrained by their spectral symmetry that most of the emerging Fermi structures are trivial. For any dynamical matrix with less than six bands constrained by multiple similarities, there are no non-trivial Fermi structures possible. In the 6-band systems discussed in the main text, two non-trivial structures emerge:

- (i) A pair of 3-level imaginary 2D Fermi surfaces, which terminate on the EP2 surfaces along the EP3 arcs. The eigenvalues along these surfaces are given by  $\lambda_1 = -x$ ,  $\lambda_2 = x$ ,  $\lambda_3 = x + iy$ ,  $\lambda_4 = -x + iy$ ,  $\lambda_5 = x - iy$ , and  $\lambda_6 = -x - iy$ . The constraints on the parameters of the characteristic polynomial are given by three non-linear equations, namely  $3\kappa = 2y^2 - 3x^2$ ,  $3(\eta + \kappa^2) = y^4 + 3x^4$ , and  $\kappa^3 + 3\kappa\eta - 2\nu = -x^2(x^2 + y^2)^2$ ;
- (ii) A pair of 3-level 2D Fermi surfaces, which terminate on the EP2 surfaces along the EP3 arcs. The eigenvalues along these surfaces are given by  $\lambda_1 = -iy$ ,  $\lambda_2 = iy$ ,  $\lambda_3 = x + iy$ ,  $\lambda_4 = -x + iy$ ,  $\lambda_5 = x - iy$ , and  $\lambda_6 = -x - iy$ . The constraints on the parameters of the characteristic polynomial are given by three non-linear equations, namely  $3\kappa = 3y^2 - 2x^2$ ,  $3(\eta + \kappa^2) = 3y^4 + x^4$ , and  $\kappa^3 + 3\kappa\eta - 2\nu = y^2(x^2 + y^2)^2$ .

### Appendix C: Multiple Similarity-Induced Exceptional Structures in Four Dimensions

With the methods presented in the main text the exceptional structures induced by multiple similarities in 8-band models can be analytically described. For a given 8-band model  $H$  we define

$$\alpha = -\frac{\text{tr}(H^4)}{12} + \frac{[\text{tr}(H^2)]^2}{96}, \quad (\text{C1})$$

$$\beta = -\frac{\text{tr}(H^6)}{6\sqrt{2}} + \frac{\text{tr}(H^4)\text{tr}(H^2)}{16\sqrt{2}} - \frac{[\text{tr}(H^2)]^3}{192\sqrt{2}}, \quad (\text{C2})$$

$$\gamma = \frac{4\det(H)}{3} - \frac{\text{tr}(H^6)\text{tr}(H^2)}{36} - \frac{\text{tr}(H^4)[\text{tr}(H^2)]^2}{192} + \frac{7[\text{tr}(H^2)]^4}{9216}, \quad (\text{C3})$$

$$\delta = -\frac{\text{tr}(H^2)}{8}. \quad (\text{C4})$$

Due to the similarities present  $\alpha, \beta, \gamma, \delta \in \mathbb{R}$ , and the characteristic polynomial is given by

$$\begin{aligned} \mathcal{P}_8(\lambda) = & \lambda^8 + 4\delta\lambda^6 + 3(\alpha + 2\delta^2)\lambda^4 \\ & + (\sqrt{2}\beta + 6\alpha\delta + 4\delta^3)\lambda^2 \\ & + (\delta^4 + 3\alpha\delta^2 + \sqrt{2}\beta\delta + \frac{3}{4}\gamma), \end{aligned} \quad (\text{C5})$$

with the discriminant

$$\begin{aligned} \mathcal{D}_8 = & -746496 \left( 4\delta^4 + 12\alpha\delta^2 + \sqrt{32}\beta\delta + 3\gamma \right) \\ & \cdot \left[ \beta^2 (\beta^2 + 2\alpha^3 - 6\alpha\gamma) - \gamma (3\alpha^2 - \gamma)^2 \right]^2. \end{aligned} \quad (\text{C6})$$

With the mapping  $\lambda = \pm\sqrt{z - \delta}$  the reduced real polynomial is given by

$$\tilde{\mathcal{P}}_8(z) = z^4 + 3\alpha z^2 + \sqrt{2}\beta z + \frac{3}{4}\gamma, \quad (\text{C7})$$

which is the polynomial of a pseudo-Hermitian 4-band system. The exceptional structure of such a 4-band system is discussed in the main text, and the exceptional structure of the parent 8-band system with multiple similarities can be derived from it.

In four dimensions pairs of EP8s emerge for  $\alpha = \beta = \gamma = \delta = 0$ . These pairs of EP8s are connected by multiple exceptional structures:

- (i) 1D arcs of EP6s at  $\lambda = 0$  appear when the three constraints  $\alpha + 2\delta^2 = 0$ ,  $\sqrt{2}\beta + 6\alpha\delta + 4\delta^3 = 0$ , and  $\delta^4 + 3\alpha\delta^2 + \sqrt{2}\beta\delta + \frac{3}{4}\gamma = 0$  are fulfilled. These arcs appear if  $\tilde{\mathcal{P}}_8(z)$  has a threefold degenerate solution  $\tilde{z}_3 = \delta$ ;
- (ii) 2D surfaces of EP4s at  $\lambda = 0$  appear when the two constraints  $\sqrt{2}\beta + 6\alpha\delta + 4\delta^3 = 0$  and  $\delta^4 + 3\alpha\delta^2 + \sqrt{2}\beta\delta + \frac{3}{4}\gamma = 0$  are fulfilled. On the surface  $\tilde{\mathcal{P}}_8(z)$  has a twofold degenerate solution  $\tilde{z}_2 = \delta$ . The arcs of EP6s at  $\lambda = 0$  lie in the EP4 surfaces;
- (iii) 3D hypersurfaces of EP2s at  $\lambda = 0$  emerge for  $\delta^4 + 3\alpha\delta^2 + \sqrt{2}\beta\delta + \frac{3}{4}\gamma = 0$  are fulfilled. If this constraint is met one of the non-degenerate solutions of  $\tilde{\mathcal{P}}_8(z)$  is equal to  $\delta$ ;
- (iv) 1D arcs with pairs of EP4s emerging for  $\alpha = 0$ ,  $\beta = 0$  and  $\gamma = 0$ , given  $\delta \neq 0$ , which are the arcs with fourfold degeneracies of  $\tilde{\mathcal{P}}_8(z)$ ;
- (v) 2D surfaces hosting pairs of EP3s, defined by the constraints  $\alpha^2 + \gamma = 0$  and  $\beta^2 + 4\alpha^3 = 0$ . On these surfaces  $\tilde{\mathcal{P}}_8(z)$  has the threefold degenerate solution  $\tilde{z}_3$ , that results in pairs of EP3s if  $\tilde{z}_3 \neq \delta$ ;
- (vi) 3D hypersurfaces of pairs of EP2s, defined by the constraint  $\beta^2 (\beta^2 + 2\alpha^3 - 6\alpha\gamma) - \gamma (3\alpha^2 - \gamma)^2 = 0$ . In these hypersurfaces  $\tilde{\mathcal{P}}_8(z)$  has the twofold degenerate solution  $\tilde{z}_2$ , that results in pairs of EP2s if  $\tilde{z}_2 \neq \delta$ ;
- (vii) 2D surfaces hosting four EP2s, defined by  $\beta = 0$  and  $3\alpha^2 - \gamma = 0$ . The EP2 appear as pairs of real or purely imaginary EPs for  $\alpha < 0$ . These surfaces correspond to the pairs of real twofold degenerate solutions  $\pm\tilde{z}_R$  of  $\tilde{\mathcal{P}}_8(z)$ . For  $\alpha > 0$  the degenerate eigenvalues are complex  $\lambda_i \in \mathbb{C}$ , where  $\lambda_1 = \lambda_2^* = -\lambda_3 = -\lambda_4^*$ . These surfaces correspond to the pairs of imaginary degenerate solutions  $\pm\tilde{z}_I$  of  $\tilde{\mathcal{P}}_8(z)$ .

These exceptional structures are not necessarily separate from each other. Intersections between different structures result in special arcs or surfaces and for the 8-band model these are given by:

- (viii) 1D arcs with an EP4 at  $\lambda = 0$ , and a pair of real or purely imaginary EP2s, defined by  $\sqrt{2}\beta + 6\alpha\delta + 4\delta^3 = 0$ ,  $\delta^4 + 3\alpha\delta^2 + \sqrt{2}\beta\delta + \frac{3}{4}\gamma = 0$  and  $3\alpha + 2\delta^2 = 0$ , respectively. For  $\delta < 0$  the EP2s are real, and for  $\delta > 0$  the EP2s are imaginary;

- (ix) A 2D surface of EP4s at  $\lambda = 0$ , and a pair of real or purely imaginary EP2s given by  $\beta^2 (\beta^2 + 2\alpha^3 - 6\alpha\gamma) - \gamma (3\alpha^2 - \gamma)^2 = 0$  and  $\delta^4 + 3\alpha\delta^2 + \sqrt{2}\beta\delta + \frac{3}{4}\gamma = 0$ ;
- (x) A 1D arc of EP2s at  $\lambda = 0$ , and a pair 1D arcs of real or purely imaginary EP3s. The constraints that define these arcs are  $\delta^4 + 3\alpha\delta^2 + \sqrt{2}\beta\delta + \frac{3}{4}\gamma = 0$ ,

$$\alpha^2 + \gamma = 0 \text{ and } \beta^2 + 4\alpha^3 = 0, \text{ respectively.}$$

The list of the simple exceptional structures together with the list of possible intersections between them exhaustively cover the exceptional structure induced by multiple similarities in 8-band models in four dimensions. Upon adding a ninth band, the degeneracies appearing at  $\lambda = 0$  increases by one, while the remaining are left unaltered.